J|A|C|S
ARTICLES
Published on Web 10/12/2002

# 2-Aminopurine: A Probe of Structural Dynamics and Charge Transfer in DNA and DNA:RNA Hybrids

Melanie A. O'Neill and Jacqueline K. Barton*

*Contribution from the Division of Chemistry and Chemical Engineering, California Institute of Technology, Pasadena, California 91125*

Received June 10, 2002

***Abstract:*** Spectroscopic techniques are employed to probe relationships between structural dynamics and charge transfer (CT) efficiency in DNA duplexes and DNA:RNA hybrids containing photoexcited 2-aminopurine (Ap*). To better understand the variety of interactions and reactions, including CT, between Ap* and DNA, the fluorescence behavior of Ap* is investigated in a full series of redox-inactive as well as redox-active assemblies. Thus, Ap* is developed as a dual reporter of structural dynamics and base−base CT reactions in nucleic acid duplexes. CD, NMR, and thermal denaturation profiles are consistent with the family of DNA duplexes adopting a distinct conformation versus the DNA:RNA hybrids. Fluorescence measurements establish that the d(A)−r(U) tract of the DNA:RNA hybrid exhibits enhanced structural flexibility relative to that of the d(A)−d(T) tract of the DNA duplexes. The yield of CT from either G or 7-deazaguanine (Z) to Ap* in the assemblies was determined by comparing Ap* emission in redox-active G- or Z-containing duplexes to otherwise identical duplexes in which the G or Z is replaced by inosine (I), the redox-inactive nucleoside analogue. Investigations of CT not only demonstrate efficient intrastrand base−base CT in the DNA:RNA hybrids but also reveal a distance dependence of CT yield that is more shallow through the d(A)−r(U) bridge of the A-form DNA:RNA hybrids than through the d(A)−d(T) bridge of the B-form DNA duplexes. The shallow distance dependence of intrastrand CT in DNA:RNA hybrids correlates with the increased conformational flexibility of bases within the hybrid duplexes. Measurements of interstrand base−base CT provide another means to distinguish between the A- and B-form helices. Significantly, in the A-form DNA:RNA hybrids, a similar distance dependence is obtained for inter- and intrastrand reactions, while, in B-DNA, a more shallow distance dependence is evident with interstrand CT reactions. These observations are consistent with evaluations of intra- and interstrand base overlap in A- versus B-form duplexes. Overall, these data underscore the sensitivity of CT chemistry to nucleic acid structure and structural dynamics.

## Introduction

The resemblance of the array of aromatic bases in the DNA double helix to conductive, one-dimensional aromatic crystals prompted the suggestion, almost 40 years ago, that the DNA $\pi$-stack might facilitate charge transfer (CT).[1] Today, while there is a developing consensus regarding the existence and importance of long-range DNA CT,[2−5] mechanistic descriptions of *how* charge migrates through DNA provide the focus of ongoing experimental and theoretical investigations.[7−14] Questions concerning DNA CT have been addressed on a molecular level by

* To whom correspondence should be addressed: jkbarton@caltech.edu.

(1) (a) Eley, D. D.; Spivey, D. I. *Faraday Soc. Trans.* **1962**, *58*, 411−415. (b) Hoffman, T. A.; Ladik, J. *Adv. Chem. Phys.* **1964**, *7*, 84−158.
(2) (a) Núñez, M. E.; Barton, J. K. *Curr. Opin. Chem. Biol.* **2000**, *4*, 199−206. (b) Núñez, M. E.; Hall, D. B.; Barton, J. K. *Chem. Biol.* **1999**, *6*, 85−97. (c) Kelley, S. O.; Barton, J. K. *Met. Ions Biol. Syst.* **1999**, *36*, 211−249. (d) Holmlin, R. E.; Dandliker, P. J.; Barton, J. K. *Angew. Chem., Int. Ed. Engl.* **1997**, *36*, 2715−2730.
(3) Lewis, F. D.; Letsinger, R. L.; Wasielewski, M. R. *Acc. Chem. Res.* **2001**, *34*, 159−170.
(4) (a) Schuster, G. B. *Acc. Chem. Res.* **2000**, *33*, 253−260. (b) Henderson, P. T.; Jones, D.; Hampikian, G.; Kan, Y. Z.; Schuster, G. B. *Proc. Natl. Acad. Sci. U.S.A.* **1999**, *96*, 8353−8358.
(5) (a) Giese, B. *Acc. Chem. Res.* **2000**, *33*, 631−636. (b) Giese, B.; Wessely, S.; Spormann, M.; Lindemann, U.; Meggers, E.; Michel-Beyerle, M. E. *Angew. Chem., Int. Ed.* **1999**, *38*, 996−998. (c) Bixon, M.; Giese, B.; Wessely, S.; Langenbacher, T.; Michel-Beyerle, M. E.; Jortner, J. *Proc. Natl. Acad. Sci. U.S.A.* **1999**, *96*, 11713−11716.
(6) For recent commentaries, see: (a) Dekker, C.; Ratner, M. A. *Physics World* **2001**, *14*, 29−33. (b) Harriman, A. *Angew. Chem., Int. Ed.* **1999**, *38*, 945−949. (c) Grinstaff, M. W. *Angew. Chem., Int. Ed. Engl.* **1999**, *38*, 3629−3635. (d) Priyadarshy, S.; Risser, S. M.; Beratan, D. N. *JBIC, J. Biol. Inorg. Chem.* **1998**, *3*, 196−200. (e) Turro, N. J.; Barton, J. K. *JBIC, J. Biol. Inorg. Chem.* **1998**, *3*, 201−209. (f) Diederichsen, U. *Angew. Chem., Int. Ed. Engl.* **1997**, *36*, 2317−2319.
(7) (a) Bixon, M.; Jortner, J. *J. Am. Chem. Soc.* **2001**, *123*, 12556−12567. (b) Bixon, M.; Jortner, J. *J. Phys. Chem. A* **2001**, *105*, 10322−10328. (c) Bixon, M.; Jortner, J. *J. Phys. Chem. B* **2000**, *104*, 3906−3913. (d) Jortner, J.; Bixon, M.; Langenbacher, T.; Michel-Beyerle, M. E. *Proc. Natl. Acad. Sci. U.S.A.* **1998**, *95*, 12759−12765.
(8) (a) Berlin, Y. A.; Burin, A. L.; Siebbeles, L. D. A.; Ratner, M. A. *J. Phys. Chem. A* **2001**, *105*, 5666−5678. (b) Berlin, Y. A.; Burin, A. L.; Ratner, M. A. *J. Am. Chem. Soc.* **2001**, *123*, 260−268. (c) Grozema, F. C.; Berlin, Y. A.; Siebbeles, L. D. A. *J. Am. Chem. Soc.* **2000**, *122*, 10903−10909. (d) Berlin, Y. A.; Burin, A. L.; Ratner, M. A. *J. Phys. Chem. A* **2000**, *104*, 443−445.
(9) Bruinsma, R.; Gruner, G.; D'Orsogna, M. R.; Rudnick, J. *Phys. Rev. Lett.* **2000**, *85*, 4393−4396.
(10) (a) Conwell E. M.; Basko D. M. *J. Am. Chem. Soc.* **2001**, *123*, 11441−11445. (b) Rakhmanova, S. V.; Conwell, E. M. *J. Phys. Chem. B* **2001**, *105*, 2056−2061. (c) Conwell, E. M.; Rakhmanova, S. V. *Proc. Natl. Acad. Sci. U.S.A.* **2000**, *97*, 4556−4560.
(11) Smith, D. M. A.; Adamowicz, L. *J. Phys. Chem. B* **2001**, *105*, 9345−9354.
(12) Sumi, H.; Kakitani, T. *J. Phys. Chem. B* **2001**, *105*, 9603−9622.
(13) Olofsson J.; Larsson, S. *J. Phys. Chem. B* **2001**, *105*, 10398−10405.
(14) Li, X.; Zhang, H.; Yan, Y. *J. Phys. Chem. A* **2001**, *105*, 9563−9567.

examining thermal or photoinduced CT reactions between electron donors and acceptors mediated by and/or directly involving DNA. To date, such investigations have focused on two general themes: (*i*) spectroscopic measurement of the rates and yields of CT between donors and acceptors separated by an intervening DNA bridge[15−20] and (*ii*) evaluation of the yield of oxidative damage at guanine doublets (GG) following hole migration through DNA.[21−24] Several examples of time-resolved measurements of fast ($k \approx 10^6-10^8$ s$^{-1}$) and ultrafast ($k \approx 10^9-10^{12}$ s$^{-1}$) DNA-mediated CT reactions involving covalently tethered metallointercalators, organic intercalators or end-caps, and DNA bases now exist. Similarly, countless investigations have demonstrated long-range oxidative damage to GG sites within DNA, including DNA-mediated oxidation over distances as far as 200 Å.[2b,4b] As a result, it is now generally accepted that charges can migrate rapidly and over significant distances through the DNA $\pi$-stack.

DNA-mediated CT is not yet, however, well-characterized mechanistically. Of particular debate is the distance dependence of CT processes in DNA,[15b−f,16d,f,17a,18b,19c] often represented by $\beta$.[25] One explanation for the apparent disparity found in measurements of the CT distance dependence is that different experimental assemblies might operate within different regimes of a mechanistic continuum between one-step superexchange and multistep hopping.[7a,d] Irrespective of mechanism, however, DNA structural dynamics may modulate interactions between donor and acceptor and within the DNA bridge, thereby affecting the efficiency of CT. The role of structural dynamics in DNA CT has received considerably less attention than other mechanistic issues.

The significance of a donor−DNA−acceptor structure, particularly base stacking within the assembly, is one of the most important themes that has emerged from studies of DNA CT conducted in our laboratories. Investigations of oxidative damage to GG sites have definitively established the occurrence of long-range DNA-mediated CT and have consistently demonstrated the remarkable sensitivity of these reactions to the integrity of the $\pi$-stack.[21] Experiments in which base stacking interactions are altered by, for instance, mismatches,[21a,26] sequence variation,[21b] structural perturbations[21f] or protein binding,[27] emphasize how subtle changes in base stacking dramatically affect CT through DNA. Recent studies of CT in nonB-form DNA structures such as single strands,[16e,19d,28a] triplexes,[28b,c] crossover junctions,[28d] DNA:RNA hybrids[28e,f] and Z-DNA[28g] reveal also the sensitivity of CT to structural variations. Likewise, direct spectroscopic observation of CT reactions in DNA confirms that rapid, long-range CT is possible and that a well-coupled $\pi$-stack involving the redox participants and the DNA bases is indeed requisite to DNA-mediated CT.[15] While a description of long-range DNA-mediated CT must incorporate strong stacking interactions, it is equally important to emphasize that these stacking interactions are not static but are modulated by structural dynamics. Time-resolved investigations of ethidium-modified DNA duplexes established that dynamic variations in stacking are crucial to DNA CT processes and suggest that base motions may serve to gate CT.[15d]

Photoexcited 2-aminopurine (Ap*) can serve both as a sensitive probe of DNA structural dynamics and as a participant in CT reactions with DNA bases. The utility of Ap* as a probe of the DNA environment is illustrated in the diverse array of studies, including investigations of abasic sites, protein/DNA interactions, and the inclusion of nonnatural base surrogates within DNA.[29] Investigations of DNA-mediated CT benefit from the ability of Ap* to probe base−base CT in structurally well-defined DNA assemblies unperturbed by auxiliary redox reagents. Thus, while the vast majority of spectroscopic and biochemical investigations of DNA-mediated CT employ pen-


(15) (a) Wagenknecht, H. A.; Rajski, S. R.; Pascaly, M.; Stemp, E. D. A.; Barton, J. K. *J. Am. Chem. Soc.* **2001**, *123*, 4400−4407. (b) Wan, C. Z.; Fiebig, T.; Schiemann, O.; Barton, J. K.; Zewail, A. H. *Proc. Natl. Acad. Sci. U.S.A.* **2000**, *97*, 14052−14055. (c) Kelley, S. O.; Barton, J. K. *Science* **1999**, *283*, 375−381. (d) Wan, C. Z.; Fiebig, T.; Kelley, S. O.; Treadway, C. R.; Barton, J. K.; Zewail, A. H. *Proc. Natl. Acad. Sci. U.S.A.* **1999**, *96*, 6014−6019. (e) Kelley, S. O.; Barton, J. K. *Chem. Biol.* **1998**, *5*, 413−425. (f) Kelley, S. O.; Holmlin, R. E.; Stemp, E. D. A.; Barton, J. K. *J. Am. Chem. Soc.* **1997**, *119*, 9861−9870. (g) Murphy, C. J.; Arkin, M. R.; Jenkins, Y.; Ghatlia, N. D.; Bossmann, S. H.; Turro, N. J.; Barton, J. K. *Science* **1993**, *262*, 1025−1029.

(16) (a) Lewis, F. D.; Liu, X. Y.; Liu, J. Q.; Miller, S. E.; Hayes, R. T.; Wasielewski, M. R. *Nature* **2000**, *406*, 51−53. (b) Lewis, F. D.; Liu, X. Y.; Liu, J. Q.; Hayes, R. T.; Wasielewski, M. R. *J. Am. Chem. Soc.* **2000**, *122*, 12037−12038. (c) Lewis, F. D.; Kalgutkar, R. S.; Wu, Y. S.; Liu, X. Y.; Liu, J. Q.; Hayes, R. T.; Miller, S. E.; Wasielewski, M. R. *J. Am. Chem. Soc.* **2000**, *122*, 12346−12351. (d) Lewis, F. D.; Wu, T. F.; Liu, X. Y.; Letsinger, R. L.; Greenfield, S. R.; Miller, S. E.; Wasielewski, M. R. *J. Am. Chem. Soc.* **2000**, *122*, 2889−2902. (e) Lewis, F. D.; Zhang, Y. F.; Liu, X. Y.; Xu, N.; Letsinger, R. L. *J. Phys. Chem. B* **1999**, *103*, 2570−2578. (f) Lewis, F. D.; Wu, T. F.; Zhang, Y. F.; Letsinger, R. L.; Greenfield, S. R.; Wasielewski, M. R. *Science* **1997**, *277*, 673−676.

(17) (a) Hess, S.; Gotz, M.; Davis, W. B.; Michel-Beyerle, M. E. *J. Am. Chem. Soc.* **2001**, *123*, 10046−10055. (b) Davis, W. B.; Naydenova, I.; Haselsberger, R.; Ogrodnik, A.; Giese, B.; Michel-Beyerle, M. E. *Angew. Chem., Int. Ed.* **2000**, *39*, 3649−3652.

(18) (a) Fukui, K.; Tanaka, K.; Fujitsuka, M.; Watanabe, A.; Ito, O. *J. Photochem. Photobiol. B* **1999**, *50*, 18−27. (b) Fukui, K.; Tanaka, K. *Angew. Chem., Int. Ed. Engl.* **1998**, *37*, 158−161.

(19) (a) Shafirovich, V.; Dourandin, A.; Geacintov, N. E. *J. Phys. Chem. B* **2001**, *105*, 8431−8435. (b) Shafirovich, V.; Cadet, J.; Gasparutto, D.; Dourandin, A.; Huang, W. D.; Geacintov, N. E. *J. Phys. Chem. B* **2001**, *105*, 586−592. (c) Shafirovich, V.; Dourandin, A.; Huang, W. D.; Luneva, N. P.; Geacintov, N. E. *Phys. Chem. Chem. Phys.* **2000**, *2*, 4399−4408. (d) Shafirovich, V.; Dourandin, A.; Huang, W. D.; Luneva, N. P.; Geacintov, N. E. *J. Phys. Chem. B* **1999**, *103*, 10924−10933.

(20) Reid, G. D.; Whittaker, D. J.; Day, M. A.; Creely, C. M.; Tuite, E. M.; Kelly, J. M.; Beddard, G. S. *J. Am. Chem. Soc.* **2001**, *123*, 6953−6954.

(21) (a) Bhattacharya, P. K.; Barton, J. K. *J. Am. Chem. Soc.* **2001**, *123*, 8649−8656. (b) Williams, T. T.; Odom, D. T.; Barton, J. K. *J. Am. Chem. Soc.* **2000**, *122*, 9048−9049. (c) Hall, D. B.; Kelley, S. O.; Barton, J. K. *Biochemistry* **1998**, *37*, 15933−15940. (d) Stemp, E. D. A.; Arkin, M. R.; Barton, J. K. *J. Am. Chem. Soc.* **1997**, *119*, 2921−2925. (e) Arkin, M. R.; Stemp, E. D. A.; Pulver, S. C.; Barton, J. K. *Chem. Biol.* **1997**, *4*, 389−400. (f) Hall, D. B.; Barton, J. K. *J. Am. Chem. Soc.* **1997**, *119*, 5045−5046. (g) Hall, D. B.; Holmlin, R. E.; Barton, J. K. *Nature* **1996**, *382*, 731−735.

(22) (a) Sartor, V.; Boone, E.; Schuster, G. B. *J. Phys. Chem. B* **2001**, *105*, 11057−11059. (b) Ly, D.; Sanii, L.; Schuster, G. B. *J. Am. Chem. Soc.* **1999**, *121*, 9400−9410. (c) Gasper, S. M.; Schuster, G. B. *J. Am. Chem. Soc.* **1997**, *119*, 12762−12771. (d) Ly, D.; Kan, Y. Z.; Armitage, B.; Schuster, G. B. *J. Am. Chem. Soc.* **1996**, *118*, 8747−8748.

(23) (a) Giese, B.; Amaudrut, J.; Köhler, A. K.; Spormann, M.; Wessely, S. *Nature* **2001**, *412*, 318−320. (b) Meggers, E.; Michel-Beyerle, M. E.; Giese, B. *J. Am. Chem. Soc.* **1998**, *120*, 12950−12955. (c) Meggers, E.; Kusch, D.; Spichty, M.; Wille, U.; Giese, B. *Angew. Chem., Int. Ed.* **1998**, *37*, 460−462.

(24) (a) Nakatani, K.; Dohno, C.; Saito, I. *Tetrahedron Lett.* **2000**, *41*, 10041−10045. (b) Nakatani, K.; Dohno, C.; Saito, I. *J. Am. Chem. Soc.* **2000**, *122*, 5893−5894. (c) Nakatani, K.; Dohno, C.; Saito, I. *J. Am. Chem. Soc.* **1999**, *121*, 10854−10855. (d) Saito, I.; Nakamura, T.; Nakatani, K.; Yoshioka, Y.; Yamaguchi, K.; Sugiyama, H. *J. Am. Chem. Soc.* **1998**, *120*, 12686−12687.

(25) Marcus, R. A.; Sutin, N. *Biochim. Biophys. Acta* **1985**, *811*, 265−322.

(26) (a) Boon, E. M.; Ceres, D. M.; Drummond, T. G.; Hill, M. G.; Barton, J. K. *Nat. Biotechnol.* **2000**, *18*, 1096−1100. (b) Kelley, S. O.; Boon, E. M.; Barton, J. K.; Jackson, N. M.; Hill, M. G. *Nucleic Acids Res.* **1999**, *27*, 4830−4837. (c) Kelley, S. O.; Jackson, N. M.; Hill, M. G.; Barton, J. K. *Angew. Chem., Int. Ed.* **1999**, *38*, 941−945.

(27) (a) Rajski, S. R.; Kumar, S.; Roberts, R. J.; Barton, J. K. *J. Am. Chem. Soc.* **1999**, *121*, 5615−5616. (b) Rajski, S. R.; Barton, J. K. *Biochemistry* **2001**, *40*, 5556−5564.

(28) (a) Kan, Y. Z.; Schuster, G. B. *J. Am. Chem. Soc.* **1999**, *121*, 10857−10864. (b) Núñez, M. E.; Noyes, K. T.; Gianolio, D. A.; McLaughlin, L. W.; Barton, J. K. *Biochemistry* **2000**, *39*, 6190−6199. (c) Kan, Y. Z.; Schuster, G. B. *J. Am. Chem. Soc.* **1999**, *121*, 11607−11614. (d) Odom, D. T.; Dill, E. A.; Barton, J. K. *Nucleic Acids Res.* **2001**, *29*, 2026−2033. (e) Odom, D. T.; Barton, J. K. *Biochemistry* **2001**, *40*, 8727−8737. (f) Sartor, V.; Henderson, P. T.; Schuster, G. B. *J. Am. Chem. Soc.* **1999**, *121*, 11027−11033. (g) Abdou, I. M.; Sartor, V.; Cao, H. C.; Schuster, G. B. *J. Am. Chem. Soc.* **2001**, *123*, 6696−6697.

dant redox reagents, which are not integral components of DNA, investigations of base−base CT in DNA involving photoexcited[15b,c,30] and photoionized[19] Ap have recently been initiated. Using Ap*, we have directly observed ultrafast base−base CT and evaluated the dependence of CT on distance, driving force, and intra- versus interstrand pathways.[15b,c] Thus, Ap* can act as a dual reporter of DNA structural dynamics and CT.

Probing CT in DNA:RNA hybrids provides a means to explore the relationships between CT and nucleic acid structure.[31] DNA:RNA hybrids are key intermediates in DNA synthesis, transcription, reverse transcription by retroviruses, and antisense therapy.[32] Moreover, structurally, DNA:RNA hybrids are characteristically distinct from DNA duplexes. In solution, DNA:RNA hybrids exhibit a sequence-dependent range of local conformations intermediate between the A-form of RNA duplexes and the B-form of DNA duplexes.[33] The global structure tends to be closer to A-form, with the RNA strand maintaining features characteristic of A-form structures (particularly the C3′-endo sugar pucker), and the DNA strand showing more structural variety. The sequence-dependent structural dynamics of DNA:RNA hybrids are also quite distinct from DNA duplexes, as revealed by base pair lifetimes[34] and C2′OH dynamics and hydration.[35]

Studies of long-range oxidative damage at GG sites have previously revealed efficient, long-range CT through DNA:RNA hybrids.[28e,f] A reduction in the yield of oxidative damage in DNA:RNA hybrids relative to DNA duplexes was attributed to less efficient trapping within the A-form structure, rather than less efficacious CT.[28f] However, because of the nature of the experiments, it was not possible to examine charge injection and CT independently of charge trapping or to explicitly address the impact of structural dynamics.

Here, we examine the fluorescence behavior of Ap-modified nucleic acid duplexes first in redox-inactive assemblies to develop a picture of the structural dynamics within DNA and DNA:RNA duplexes and then in redox-active duplexes to probe CT. Through these combined investigations, we can establish links between CT chemistry and structural dynamics.

## Experimental Section

**Materials.** DNA oligonucleotides were synthesized on an ABI DNA Synthesizer using standard solid-phase techniques. Typically, syntheses were conducted using 2.5 $\mu$M CPG columns (Glen Research) with automatic detritylation and cleavage from the support. Incorporation of the modified nucleosides, 2-aminopurine (Ap), inosine (I), and 7-deaza-guanine (Z) was accomplished using the respective phosphoramidites, as obtained from Glen Research. In the preparation of Z-containing oligonucleotides, a mild oxidant, (*R*)-10-camphorsulfonyl oxaziridine (obtained from Aldrich and used as received) was employed. Detritylated DNA oligonucleotides were twice purified on a Hewlett-Packard HPLC using a reverse-phase C-18 column with an acetonitrile/30 mM ammonium acetate gradient (0−15% acetonitrile over 35 min) and subsequently analyzed by mass spectrometry (MALDI). After purification, the oligonucleotides were resuspended in 1 mL of Millipore water, dried via speedvac, and stored at −20 °C until use. RNA oligonucleotides were obtained from Dharmacon Research in the 2′-bis(acetoxyethoxy)-methyl ether (2′-ACE) form and deprotected and desalted immediately prior to use.

**DNA and DNA:RNA Duplexes.** DNA and RNA oligonucleotides were quantified using UV−vis spectroscopy with the following extinction coefficients for the nucleotides at 260 nm:[36] A = 15 400; G = 11 500; I = 11 000; C = 7400; T = 8700; Ap = 2500; U = 10 210 L mol$^{-1}$ cm$^{-1}$. Typically, the purified oligonucleotides were dissolved in 200−700 $\mu$L of buffer (100 mM sodium phosphate, pH 7) to generate a stock solution of the order of $10^{-4}$ M. Duplex solutions were prepared by combining equimolar amounts of the desired DNA complements (typically 20−100 $\mu$L of oligonucleotide stock solution) and diluting to the requisite volume (typically 300 $\mu$L for fluorescence experiments) with buffer. Annealing was accomplished by placing the duplex solutions at 90 °C for approximately 5 min, followed by slow cooling to 4 °C over a period of 3 h using a Thermocycler. Duplex formation was evaluated by examining the temperature-dependent absorbance of Ap at 325 nm. Duplexes containing Ap−T base pairs melt cooperatively, including the Ap region which generally begins melting less than 1−3 °C below the natural bases.[37] Melting temperatures obtained by monitoring at the Ap site, therefore, reflect the minimum temperatures for denaturation of the duplexes. The absorbance of Ap at 325 nm decreases as a result of the helix-to-coil transition, and duplex melting is thus characterized by hypochromicity of Ap. All duplexes displayed cooperative thermal denaturation profiles with melting temperatures (measured at 325 nm for 100 $\mu$M duplex samples) ≥ 14 °C (Type-1 duplexes) or ≥ 23 °C (Type-2 duplexes) and were, therefore, fully duplexed under experimental conditions (5 °C or 10 °C for Type-1 and Type-2 duplexes, respectively). The annealed duplexes were maintained at ≤10 °C prior to and during the experiment. Absorbance at the excitation wavelength (325 nm) was similar for each duplex (±<5%). The distances between Ap and the electron donor, either G or Z, were obtained from molecular models of each DNA or DNA:RNA assembly generated using commercial software (Insight II).

**Fluorescence Experiments.** Steady-state fluorescence measurements on Ap-containing DNA and DNA:RNA duplexes were conducted using an ISS K2 fluorimeter. Measurements were performed using fluorescence cells with a 5-mm path length in order to minimize inner filter effects. Emission spectra were obtained by exciting at 325 nm and monitoring the integrated emission between 340 and 500 nm. Fluorescence polarization measurements examined the polarized emission at 370 nm following excitation with polarized light at 325 nm. Excitation spectra were obtained by monitoring the emission at 370 nm while scanning excitation wavelengths between 240 and 350 nm. The duplex concentration for emission and polarization measurements was either 100 $\mu$M or 50 $\mu$M, and the temperature was either 5 °C (Type-1 duplexes) or 10 °C (Type-2 duplexes). The duplex concentration for excitation experiments was 5 $\mu$M. This reduction in duplex

(29) (a) Rachofsky, E. L.; Seibert, E.; Stivers, J. T.; Osman, R.; Ross, J. B. A. *Biochemistry* **2001**, *40*, 957−967. (b) Stivers, J. T. *Nucleic Acids Res.* **1998**, *26*, 3837−3844. (c) Holz, B.; Klimasauskas, S.; Serva, S.; Weinhold, E. *Nucleic Acids Res.* **1998**, *26*, 1076−1083. (d) Allan, W. B.; Reich, N. O. *Biochemistry* **1996**, *35*, 14757−14762. (e) Mandal, S. S.; Fidalgo da Silva, E.; Reha-Krantz, L. J. *Biochemistry* **2002**, *41*, 4399−4406. (f) Hochstrasser, R. A.; Carver, T. E.; Sowers, L. C.; Millar, D. P. *Biochemistry* **1994**, *33*, 11971−11979. (g) Singh, I.; Hecker, W.; Prasad, A. K.; Parmar, V. S.; Seitz, O. *Chem. Commun.* **2002**, 500−501.

(30) Larsen, O. F. A.; van Stokkum, I. H. M.; Gobets, B.; van Grondelle, R.; van Amerongen, H. *Biophys. J.* **2001**, *81*, 1115−1126.

(31) (a) Saenger, W. *Principles of Nucleic Acid Structure;* Springer-Verlag: New York, 1984. (b) Hartman, B.; Lavery, R.; *Q. Rev. Biophys.* **1996**, *29*, 309−368.

(32) (a) Adams, R. L. P.; Knowler, J. T.; Leader, D. P. *The Biochemistry of Nucleic Acids*, 10th ed.; Chapman and Hall: London, 1986; Chapter 6. (b) Hansen, U. M.; McClure, W. R. *J. Biol. Chem.* **1980**, *255*, 9564−9570. (c) Varmus, H. *Science* **1988**, *240*, 1427−1435. (d) Stephenson, M. L.; Zamenick, P. C. *Proc. Natl. Acad. Sci. U.S.A.* **1978**, *75*, 285−288.

(33) (a) Gyi, J. I.; Lane, A. N.; Conn, G. L.; Brown, T. *Biochemistry* **1998**, *37*, 73−80. (b) Gyi, J. I.; Conn, G. L.; Lane, A. N.; Brown, T. *Biochemistry* **1996**, *35*, 12538−12548. (c) Fedoroff, O. Y.; Salazar, M.; Reid, B. R. *J. Mol. Biol.* **1993**, *233*, 509−523.

(34) (a) Snoussi, K.; Leroy, J.-L. *Biochemistry* **2001**, *40*, 8898−8904. (b) Maltseva, T. V.; Zarytova, V. F.; Chattopadhyaya, J. *J Biochem. Biophys. Methods* **1995**, *30*, 163−177.

(35) Gyi, J. I.; Lane, A. N.; Conn, G. L.; Brown, T. *Nucleic Acids Res.* **1998**, *26*, 3104−3110.

(36) Bover, P. N. *Handbook of Biochemistry and Molecular Biology;* CRC Press, 1975.

(37) (a) Eritja, R.; Kaplan, B. E.; Mhaskar, D.; Sowers, L. C.; Petruska, J.; Goodman, M. F. *Nucleic Acids Res.* **1986**, *14*, 5869−5885. (b) Xu, D. G.; Evans, K. O.; Nordlund, T. M. *Biochemistry* **1994**, *33*, 9592−9599.

concentration is necessary, since the natural DNA bases, which are in greater abundance and have a much higher extinction coefficient than that of Ap at 260 nm, absorb the lower wavelength (<300 nm) light very strongly. Excitation spectra were obtained at 5 °C. In 100 mM sodium phospshate buffer, 5 $\mu$M samples of most Type-1 and all Type-2 duplexes melt above 15 °C and fluorescence spectra recorded at 5 °C represent fully duplexed samples.

Evaluation of the yield of CT from emission spectra is accomplished by comparing the observed fluorescence intensity in redox-active G- or Z-containing duplexes to those of otherwise identical duplexes in which the G or Z is replaced by inosine (I), an analogue of G and Z which is inactive toward the electron transfer (ET) quenching of Ap*. It is necessary to employ a redox-inactive reference in order to account for the subtle influences of an oligonucleotide sequence and duplex environment on the fluorescence of Ap and, therefore, accurately quantify fluorescence quenching due to CT. The fraction of fluorescence quenching due to CT from G or Z to photoexcited Ap is thus quantified as $F_q$, where $F_q = 1 - \Phi_{rG/Z}/\Phi_{rI}$. The evaluation of $F_q$ is based on the quantum yields for a pair of duplexes (I and G or Z duplexes) measured in a single experiment. The average $F_q$ is thus determined from replicate measurements, and the standard deviation is determined from the variation in individual $F_q$ values.

Fluorescence lifetimes of Ap in DNA and DNA:RNA duplexes were obtained using a ps laser system previously described.[38] Duplex samples (100 $\mu$M) were excited with 355-nm laser light from a regeneratively amplified mode-locked Nd:YAG laser at room temperature. The emission was monitored with a streak camera at wavelengths > ~370 nm for a total time of 10 ns or 50 ns. The instrument response function (IRF) values in these two regimes were 205 and 542 ps, respectively. For redox-inactive duplexes, the emission decay traces observed over the 50-ns time regime were fit to a double first-order exponential expression without deconvolution of the instrument response ($f(t) = \alpha_1\exp(-t/\tau_1) + \alpha_2\exp(-t/\tau_2)$), yielding two lifetimes and their corresponding contribution to the overall decay. The multiexponential decay of Ap fluorescence in duplex DNA (commonly fit to 4 exponentials) can be observed on significantly shorter time scales than those accessible in the current experiments. The lifetimes reported herein represent the longest lifetime components.

**CD and UV−vis Measurements.** CD spectra were obtained on an Aviv CD spectrometer at 10 °C. The duplex concentration for CD experiments was 2.5 $\mu$M. UV spectra were obtained on a Beckman UV−vis spectrometer operating at room temperature (single strands) or 10 °C (duplexes). The melting profiles of the duplexes were obtained by slowly lowering the temperature (0.5 °C min$^{-1}$) from 75 °C to 10 °C and measuring the absorbance at a single wavelength (either 260 or 325 nm) at each temperature. The concentration of a duplex was either 100 $\mu$M or 50 $\mu$M when monitoring Ap absorbance at 325 nm or 5 $\mu$M when monitoring the absorbance of the natural DNA bases at 260 nm. The $T_m$ values represent the midpoint of the transition as obtained by fitting the melting profiles with a sigmoidal expression in Origin.

**Transient Absorption.** Transient absorption measurements were made using a YAG-OPO laser ($\lambda_{ex}$ = 310 nm, 0.5−1.0 mJ/pulse) as previously described.[15a] Transient absorption spectra were generated by fitting individual decay traces at a given wavelength to a first-order exponential function, and the absorbance changes were derived by extrapolating these fits to time zero. The spectrum of the guanine radical was obtained using solutions of 100 $\mu$M Ap and 50 mM dGTP in aerated 100 mM sodium phosphate buffer at pH 7.

**NMR Spectroscopy.** Two-dimensional NOESY spectra of $D_2O$ solutions of DNA and DNA:RNA duplexes (~0.5 mM) were recorded on a Varian INOVA 600 MHz spectrometer at 288 K using presaturation of the residual water signal. The conditions used in spectral acquisition were the following: 600 MHz, 8-ppm sweep widths, 2048 complex points, hypercomplex mode, 256 $t_1$ blocks, 32 scans per $t_2$ block, 1.5-s relaxation delay, 150-ms mixing time. Linear prediction was employed in the indirect dimension in order to increase resolution near the diagonal. All two-dimensional processing was carried out using VNMR 6.1b software (Varian) on a SUN station. Chemical shifts are reported relative to the internal standard, sodium 3-trimethylsilyl-[2,2,3,3-D4] propionate (TMSP).

***Scheme 1.*** Nucleoside Analogues and Corresponding Natural Nucleosides Employed in This Study

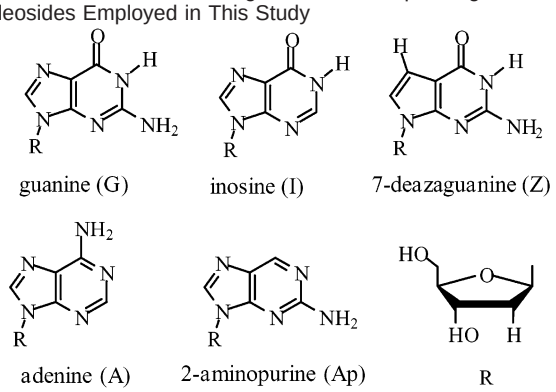


## Results

**DNA and DNA:RNA Assemblies Containing Ap.** The DNA and DNA:RNA duplexes employed possess Ap as well as additional base analogues in order to tune the photophysics and redox characteristics of the duplexes with minimal structural impact (Scheme 1). The specific sequences utilized are presented in Table 1. Each DNA or DNA:RNA duplex contains Ap paired with thymine (T) or uracil (U) on the complementary strand. Investigations of the structure and stability of Ap-containing DNA duplexes by NMR, fluorescence spectroscopy, and calorimetry have shown that Ap undergoes normal Watson−Crick pairing with T and is well-stacked within the DNA helix in a manner which is similar to adenine.[37,39] Because of the unique photophysics of Ap relative to natural DNA bases,[40,41] it is possible to selectively excite Ap in DNA duplexes.

Two general types of duplexes were employed. Type-1 duplexes possess a purine-deficient RNA strand (21−36% purine), while the Type-2 duplexes possess a purine-rich RNA strand (56−69% purine). In all cases, Ap is positioned on the DNA strand. In addition, Ap is separated from I, G or Z by a d(A)−d(T) DNA bridge, or a d(A)−r(U) DNA:RNA bridge.

Our previous investigations of base−base CT demonstrate that both guanine (G) and 7-deaza-guanine (Z) transfer an electron to Ap* in solution and in DNA duplexes, resulting in fluorescence quenching.[15b,c] Thymine (T), cytosine (C), and the analogue inosine (I) do not undergo this oxidative CT reaction with photoexcited Ap[15c] (although T and C may react via reductive CT with Ap* in DNA[15b]). These observations are

(38) Lyubovitsky, J. G.; Gray, H. B.; Winkler, J. R. *J. Am. Chem. Soc.* **2002**, *124*, 5481−5485.

(39) (a) Nordlund, T. M.; Andersson, S.; Nilsson, L.; Rigler, R.; Gräslund, A.; McLaughlin, L. W. *Biochemistry* **1989**, *28*, 9095−9103. (b) Guest, C. R.; Hochstrasser, R. A.; Sowers, L. C.; Millar, D. P. *Biochemistry* **1991**, *30*, 3271−3279. (c) Law, S. M.; Eritja, R.; Goodman, M. F.; Breslauer, K. J. *Biochemistry* **1996**, *35*, 12329−12337.

(40) Ward, D. C.; Reich, E.; Stryer, L. *J. Biol. Chem.* **1969**, *244*, 1228−1237.

(41) (a) Smagowicz, J.; Wierzchowski, K. L. *J. Lumin.* **1974**, *8*, 210−232. (b) Santhosh, C.; Mishra, P. C. *Spectrochim. Acta* **1991**, *47A*, 1685−1693. (c) Holmen, A.; Norden, B.; Albinsson, B. *J. Am. Chem. Soc.* **1997**, *119*, 3114−3121. (d) Broo, A. *J. Phys. Chem. A* **1998**, *102*, 526−531. (e) Nir, E.; Kleinermanns, K.; Grace, L.; de Vries, M. S. *J. Phys. Chem. A* **2001**, *105*, 5106−5110.

***Table 1.*** Assemblies Employed for Investigations of Intra- and Interstrand Base−Base CT in DNA and DNA:RNA Duplexes

| Ap-DNA strand | DNA or RNA complement | label |
|---|---|---|
| | intrastrand CT Type-1; Y = I, Z | |
| 5′-T A I **Ap Y** I T I T T A T I A | 3′-A T C T C C A C A A T A C T | $ApA_0Y$-1 |
| | 3′-a u c u c c c a c a a u a c u | $apa_0y$- 1 |
| 5′-T A I **Ap A Y** I T A T T A I A | 3′-A T C T T C C A T A A T C T | $ApA_1Y$-1 |
| | 3′-a u c u u c c a u a a u c u | $apa_1y$-1 |
| 5′-T A I **Ap A A Y** I T I T A I A | 3′-A T C T T T C C A C A T C T | $ApA_2Y$-1 |
| | 3′-a u c u u u c c a c a u c u | $apa_2y$-1 |
| 5′-T A I **Ap A A A Y** I T A T I A | 3′-A T C T T T T C C A T A C T | $ApA_3Y$-1 |
| | 3′-a u c u u u u c c a c a c u | $apa_3Y$-1 |
| | intrastrand CT Type-2; Y = I, G | |
| 5′-T C T I **Ap Y** I T C T A T C T C T | 3′-A I A C T C C A I A T A I A I A | $ApA_0Y$-2 |
| | 3′-a i a c u c c a i a u a i a i a | $apa_0y$-2 |
| 5′-T C T I **Ap A Y** I T C T A T T C T | 3′-A I A C T T C C A I A T A A I A | $ApA_1Y$-2 |
| | 3′-a i a c u u c c a i a u a a i a | $apa_1y$-2 |
| 5′-T C T I **Ap A A Y** I T C T A T C T | 3′-A I A C T T T C C A I A T A I A | $ApA_2Y$-2 |
| | 3′-a i a c u u u c c a i a u a i a | $apa_2y$-2 |
| 5′-T C T I **Ap A A A Y** I T C T T C T | 3′-A I A C T T T T C C A I A A I A | $ApA_3Y$-2 |
| | 3′-a i a c u u u u c c a i a a i a | $apa_3y$-2 |
| | interstrand CT; Y= I, G | |
| 5′-T C T I **Ap C** I T C T A T C T C T | 3′-A I A C **T Y** C A I A T A I A I A | $ApA_0C$-$YT_1$ |
| | 3′-a i a c **u y** c a i a u a i a i a | $apa_0c$-$yu_1$ |
| 5′-T C T I **Ap A C** I T C T A T T C T | 3′-A I A C **T T Y** C A I A T A A I A | $ApA_1C$-$YT_2$ |
| | 3′-a i a c **u u y** c a i a u a a i a | $apa_1c$-$Yu_2$ |
| 5′- T C T I **Ap A A C** I T C T A T C T | 3′-A I A C **T T T Y** C A I A T A I A | $ApA_2C$-$YT_3$ |
| | 3′-a i a c **u u u y** c a i a u a i a | $apa_2c$-$yu_3$ |
| 5′-T C T I **Ap A A A C** I T C T T C T | 3′-A I A C **T T T T Y** C A I A A I A | $ApA_3C$-$YT_4$ |
| | 3′-a i a c **u u u u y** c a i a a i a | $apa_3c$-$yu_4$ |

consistent with the driving forces for oxidative CT which are ∼200 mV and 500 mV for G and Z, respectively, and thermodynamically unfavorable for the other nucleotides.[15c,e] Consequently, redox-active DNA and DNA:RNA duplexes for CT investigations contain Ap systematically separated from either G or Z by the d(A)−d(T) or d(A)−r(U) base pairs, with the remaining sequence constructed of I−C or A−T(A−U) pairs that do not undergo significant oxidative CT with Ap*. Measurements of oxidative CT reactions in each DNA or DNA:RNA duplex were calibrated against an otherwise identical duplex in which the electron donor, G or Z, has been replaced by the redox-inactive I.

Considerable experimental evidence correlates DNA:RNA hybrid structure and stability with the percentage of purines on the RNA strand.[33a,b,42] The Type-2 hybrid duplexes thus are expected to exhibit enhanced thermodynamic stability and A-form character. As a result, assemblies for investigating interstrand CT reactions were based on the Type-2 design. These assemblies differ from those employed in intrastrand CT investigations only by the exchange of the bases in one base pair between the two oligonucleotide strands.

**Characterization of Ap-Modified DNA Duplexes and DNA:RNA Hybrids.** In solution, DNA:RNA hybrid duplexes are best described as a composite of B-form and A-form structures.[33] As a general rule, the RNA strand maintains most features characteristic of the A-form structure (e.g., C3′-endo sugar pucker and glycosidic bond torsion angles), while the DNA strand exhibits considerably more variation and flexibility. Significantly, the extent of A and B conformation at both the nucleotide and duplex level is a sensitive function of the oligonucleotide sequence. The DNA duplexes and analogous DNA:RNA hybrids utilized here were, therefore, characterized by a combination of CD, NMR and UV−Vis spectroscopy (thermal denaturation), and steady-state and time-resolved fluorescence. DNA and DNA:RNA duplexes containing Ap are particularly amenable to investigation, as the optical spectroscopy of Ap is a sensitive probe of oligomer environment, local structure, and structural dynamics.[29,37b,39,43,44]

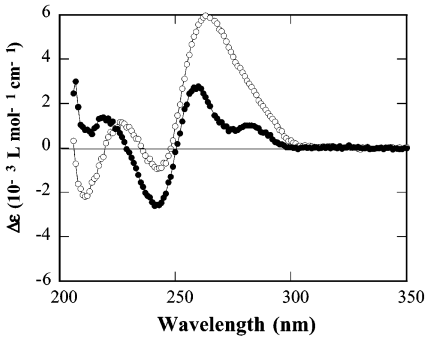


***Figure 1.*** CD spectra of DNA duplexes (closed circles) and DNA:RNA hybrids (open circles) of Type-2 $ApA_0G$-2 and $apa_0g$-2 assemblies. The spectra were obtained at 10 °C using 5 $\mu$M duplexes in 100 mM sodium phosphate buffer at pH 7.

**CD Spectroscopy.** Representative CD spectra of Type-2 DNA duplexes and analogous DNA:RNA hybrids are shown in Figure 1. Additional CD spectra are presented in the Supporting Information. As anticipated, the DNA duplexes exhibit positive bands between 250 and 300 nm and near 220 nm, as well as a negative band near 245 nm, characteristic of the B-form DNA structure.[45a] The DNA:RNA hybrids similarly

(42) (a) Lesnik, E. A.; Freier, S. M. *Biochemistry* **1995**, *34*, 10807−10815. (b) Ratmeyer, L.; Vinayak, R.; Zhong, Y. Y.; Zon, G.; Wilson, W. D. *Biochemistry* **1994**, *33*, 5298−5304.

(43) Rachofsky, E. L.; Osman, R.; Ross, J. B. A. *Biochemistry* **2001**, *40*, 946−956.

(44) (a) Xu, D. G.; Nordlund, T. M. *Biophys. J.* **2000**, *78*, 1042−1058. (b) Nordlund, T. M.; Xu, D. G.; Evans, K. O. *Biochemistry* **1993**, *32*, 12090−12095.

(45) (a) Gray, D. M.; Ratliff, R. L.; Vaughan, M. R. *Methods Enzymol.* **1992**, *211*, 389−406. (b) Gray, D. M.; Hung, S. H.; Johnson, K. H. *Methods Enzymol.* **1995**, *246*, 19−34.

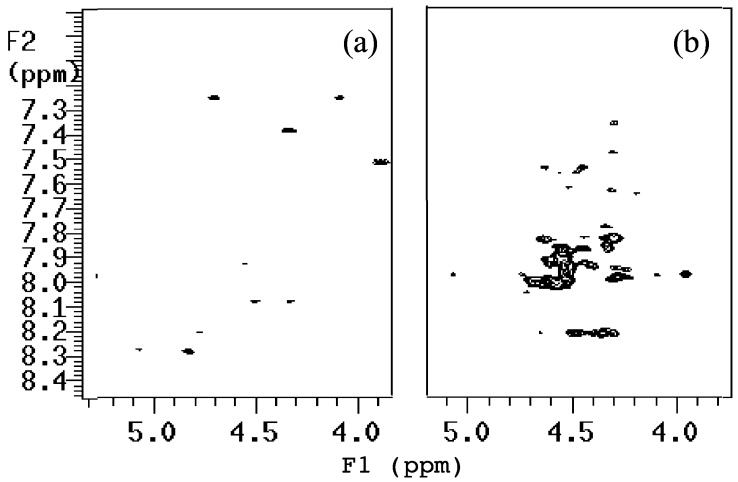


***Figure 2.*** Two-dimensional $^1$H NMR spectra of (a) the DNA duplex, $ApA_1Z$-1, and (b) the DNA:RNA duplex, $apa_1z$-1. Shown is the contour plot of aromatic and sugar H3′ region of a 150-ms NOESY spectrum at 288 K of (a) ApAZ-1 and (b) apaz-1 in 100 mM sodium phosphate buffer at pD 7.0, in 100% $D_2O$ with TMSP as standard.

exhibit CD bands with positive maxima near 270 and 220 nm, as well as a negative maximum at 240 nm. For the Type-1 assemblies, the peak positions of the DNA:RNA hybrids are not significantly shifted relative to the DNA duplexes. However, the intensity of the positive peak near 270 nm is notably larger in the DNA:RNA hybrids than in pure B-form DNA duplexes. In addition, the DNA:RNA hybrids are characterized by a second negative CD band near 210 nm. The differences in CD spectra between the Type-2 DNA duplexes and DNA:RNA hybrids are even more dramatic (Figure 1). For these assemblies, the CD bands of the DNA:RNA hybrids are distinct from those of the DNA duplexes in position and shape, and the negative CD band of the hybrids at 210 nm is more pronounced. Furthermore, the significant difference in molar ellipticities between the DNA duplexes and the DNA:RNA hybrids, both near 270 and 245 nm, is striking.

The differences in the CD spectra indicate that the global structure of each DNA:RNA hybrid is distinct from the analogous DNA duplex and that the DNA:RNA hybrids adopt a significant degree of A-conformation in solution. The negative band at 210 nm and the enhanced positive ellipticity between 250 and 300 nm are characteristic CD spectral features which distinguish A-RNA from B-DNA.[45b] The structures and characteristics of these hybrid duplexes lie in a continuum between idealized A and B conformations, albeit generally more A-like than B-like.[33a,b,42] Moreover, a progressive increase in A-form conformation is generally observed as the concentration of purines on the RNA strand is increased. The difference in the CD spectra between the Type-1 and Type-2 DNA:RNA hybrids is consistent with these observations.

More subtle variations are also detected. Specifically, the CD spectra of the Type-1 and Type-2 assemblies are distinct, and the spectra of duplexes possessing ApY motifs are different from those of duplexes possessing $Ap(A)_nY$ motifs (Supporting Information). These variations, observed in both DNA and DNA:RNA duplexes, reflect the different sequence arrangement of the Type-1 and Type-2 assemblies and the variation in stacking interactions and helical parameters among different sequences such as ApY and ApAAAY. An important comparison is also made between the CD spectra of the redox-active and redox-inactive duplexes. Substitution of a single I for either G or Z causes no detectable change in the CD spectra of the DNA duplexes or the DNA:RNA hybrids (Supporting Information). This is consistent with the structural similarity of I, G, and Z. Nonetheless, these data support the premise that I substitution represents a minor structural perturbation and that I-substituted duplexes are indeed fair references for CT investigations in redox-active duplexes (vide infra).

**NMR Spectroscopy.** Confirmation that the DNA:RNA hybrids exist in A-like conformations can be obtained using 2D-NMR spectroscopy.[33a,b] Through-space NOEs obtained from NOESY spectra can be used to evaluate intra- and internucleotide distances in oligonucleotide duplexes.[46] For instance, the internucleotide distance between the sugar H3′ and the aromatic H6 or H8 protons of the adjacent bases in B-DNA is too long to generate observable NOEs; in A-form structures, this distance is sufficiently shortened to produce a measurable NOE in the NOESY spectra. As can clearly be seen in Figure 2, internucleotide coupling between sugar H3′ and base H6 and H8 protons, which are distinctly absent in the B-DNA duplexes, are dramatically evident in the DNA:RNA hybrids.

**UV−vis Spectroscopy and Thermal Denaturation.** The duplex melting temperature ($T_m$) and hypochromicity of Ap observed upon thermal denaturation of the DNA duplexes and analogous DNA:RNA hybrids employed in intrastrand CT investigations are presented in Table 2. The corresponding interstrand CT assemblies exhibit essentially identical $T_m$ values and hypochromicities. Several interesting features are apparent in the $T_m$ data. First, the melting temperatures of the Z- or G-containing duplexes are up to 6 °C higher than those of the corresponding I-containing duplexes for both B-DNA and the DNA:RNA hybrids. This is consistent with $T_m$ values observed in other I-containing DNA duplexes.[47]

Second, the DNA:RNA hybrids consistently melt at lower temperatures than the DNA analogues. This is not unexpected on the basis of previous investigations.[33b,42,48] More interesting, however, is the fact that the $T_m$ values of the DNA:RNA duplexes containing either I, Z, or G decrease as the number of

(46) Wüthrich, K. *NMR of Proteins and Nucleic Acids*; Wiley: New York, 1986.
(47) Kelley, S. O.; Treadway, C. R. Unpublished results in our laboratory.
(48) (a) Hall, K. B.; Mclaughlin, L. W. *Biochemistry* **1991**, *30*, 10606−10613. (b) Roberts, W. R.; Crothers, D. M. *Science* **1992**, *258*, 1463−1466.

***Table 2.*** Melting Temperatures and Ap Hypochromicities of DNA Duplexes and DNA:RNA Hybrids (100 $\mu$M Duplexes in 100 mM Sodium Phosphate Buffer at pH 7) Determined by Monitoring Absorption by Ap at 325 nm from 75−10 °C[a]

| DNA duplex | $T_m$/°C (% hypochromicity) | DNA:RNA duplex | $T_m$/°C (% hypochromicity) | $\Delta T_m$/°C |
|---|---|---|---|---|
| $ApA_0I$-1 | 29 (39) | $apa_0i$-1 | 22 (31) | 7 |
| $ApA_1I$-1 | 30 (43) | $apa_1i$-1 | 21 (28) | 9 |
| $ApA_2I$-1 | 30 (39) | $apa_2i$-1 | 15 (33) | 15 |
| $ApA_3I$-1 | 32 (38) | $apa_3i$-1 | 14 (34) | 18 |
| $ApA_0Z$-1 | 33 (37) | $apa_0z$-1 | 27 (28) | 6 |
| $ApA_1Z$-1 | 33 (43) | $apa_1z$-1 | 28 (35) | 5 |
| $ApA_2Z$-1 | 33 (43) | $apa_2z$-1 | 22 (32) | 11 |
| $ApA_3Z$-1 | 35 (42) | $apa_3z$-1 | 20 (33) | 15 |
| $ApA_0I$-2 | 32 (40) | $apa_0i$-2 | 30 (31) | 2 |
| $ApA_1I$-2 | 36 (32) | $apa_1i$-2 | 29 (24) | 7 |
| $ApA_2I$-2 | 38 (42) | $apa_2i$-2 | 25 (26) | 13 |
| $ApA_3I$-2 | 40 (41) | $apa_3i$-2 | 23 (23) | 17 |
| $ApA_0G$-2 | 38 (46) | $apa_0g$-2 | 34 (38) | 4 |
| $ApA_1G$-2 | 39 (46) | $apa_1g$-2 | 33 (31) | 6 |
| $ApA_2G$-2 | 38 (50) | $apa_2g$-2 | 29 (25) | 9 |
| $ApA_3G$-2 | 41 (52) | $apa_3g$-2 | 28 (27) | 13 |

[a] The errors in the $T_m$ values and hypochromicities are ±1 °C and ±5%, respectively. The difference in melting temperatures, DNA − DNA:RNA hybrid, is represented by $\Delta T_m$.

consecutive A−U base pairs in the duplex increases. Conversely, the DNA duplexes exhibit little variation in melting temperature with the number of consecutive A−T base pairs. Significantly, then, the difference in $T_m$ values ($\Delta T_m$) between the DNA duplexes and the DNA:RNA hybrids is a systematic one, increasing as the number of A−T/A−U base pairs separating Ap from I, Z, or G increases. Notably, the $T_m$ values of the DNA duplexes are essentially unchanged by the substitution of up to four consecutive thymine bases with deoxyuracil. Parallel observations can be made when considering the hypochromicity values. In particular, the hypochromicity of Ap, which is typically 40−50% in DNA duplexes,[37b,49] is reduced to 20−30% in the DNA:RNA hybrids.

A third observation that can be made regarding the $T_m$ data relates to the difference in $T_m$ values between the Type-1 and Type-2 assemblies. Because of the dependence of $T_m$ on oligonucleotide length, both DNA and DNA:RNA duplexes of Type-2 composition (16 mers) melt at higher temperatures than the corresponding Type-1 duplexes (14 mers). However, the difference in $T_m$ values between the two types of assemblies is consistently a few degrees larger for the DNA:RNA hybrids than the DNA duplexes. This is anticipated on the basis of previous reports correlating increased DNA:RNA hybrid stability with increased purine content on the RNA strand.[33b,42]

The position of the absorption maxima of Ap in oligonucleotide duplexes reflects the surrounding environment. In particular, free, neutral Ap has an absorption maximum near 305 nm, while Ap in duplex DNA absorbs between 310 nm and 320 nm.[37,40] The red-shifted absorption peak is comparable to the N-1 protonated form of Ap and is largely attributed to the hydrogen bonding at N-1 when Ap is base paired with T in duplex DNA.[37,49] Interestingly, subtle differences are observed between the absorption maxima of Ap in DNA and DNA:RNA duplexes. In the DNA duplexes, Ap has an absorption maximum at 320 nm, while, in the DNA:RNA duplexes, the absorption maximum of Ap is blue-shifted slightly to 317 nm. Although this difference is small, it is consistently observed for all DNA and DNA:RNA duplexes examined in this study and may be significant, considering that the maximum red-shift of Ap upon incorporation into duplex DNA is only 5−15 nm.

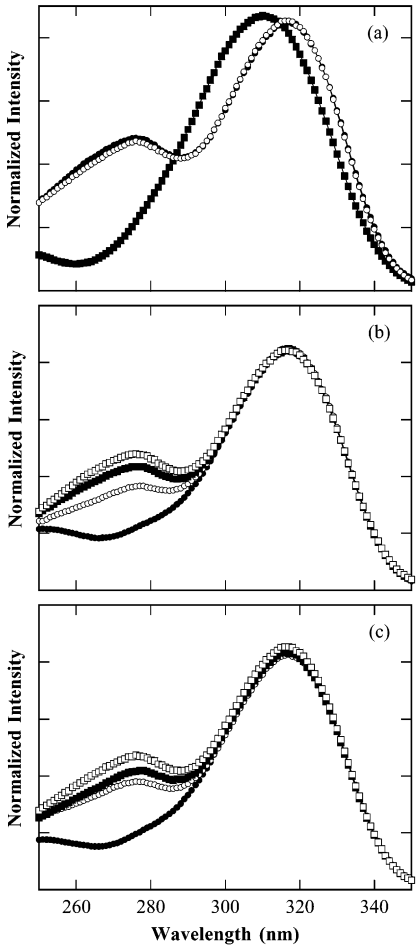


***Figure 3.*** (a) Excitation spectra of free Ap (closed squares), Ap in a DNA duplex, $ApA_3I$-2 (closed circles), and Ap in a DNA:RNA hybrid, $apa_3i$-2 (open circles). Excitation spectra as a function of $n$, $n = 0$ (closed circles), $n = 1$ (open circles), $n = 2$ (closed squares), and $n = 3$ (open squares), are shown for (b) DNA duplexes, $Ap(A)_nI$-2, and (c) DNA:RNA hybrids, $ap(a)_ni$-2. Spectra were obtained at 5 °C using 5 $\mu$M duplex samples in 100 mM sodium phosphate buffer at pH 7.

**Fluorescence Investigations of Ap-Modified Duplexes as a Probe of Structure and Structural Dynamics.** The fluorescence of Ap* sensitively probes the environment of Ap in oligonucleotide duplexes.[29,39,44] Here, we focus on characterizing the fluorescence of I-containing, redox-inactive duplexes as a function of our variations in sequence and duplex structure. We note, throughout, however, consistent trends in redox-active and -inactive duplexes.

**Excitation Spectra.** One feature of the fluorescence excitation spectra diagnostic of stacking is the position of the long wavelength band corresponding to direct excitation of Ap; incorporation of Ap into oligonucleotide duplexes induces a red-shift in this band of ∼10 nm, attributed to the reduced solvent exposure associated with stacking within the duplex.[29b,39b,44] The Ap-containing duplexes employed here exhibit excitation spectra with a 7-nm red-shift relative to free, neutral Ap (Figure 3a), and the excitation spectra of Ap in DNA:RNA hybrids possess maxima which cannot be distinguished from those of DNA duplexes.

(49) Sowers, L. C.; Fazakerly, G. V.; Eritja, R.; Kaplan, B. E.; Goodman, M. F. *Proc. Natl. Acad. Sci. U.S.A.* **1986**, *83*, 5434−543.

***Table 3.*** Relative Steady-State Fluorescence Intensities, $\Phi_r$ (Relative to Free Ap), and CT Quenching Efficiencies, $F_q$, for Ap in DNA Duplexes and DNA:RNA Hybrids[a]

| DNA duplex | $\Phi_{rY=I}$ | $\Phi_{rY=G/Z}$ | $F_q$ | DNA:RNA duplex | $\Phi_{rY=I}$ | $\Phi_{rY=G/Z}$ | $F_q$ |
|---|---|---|---|---|---|---|---|
| $ApA_0Y$-1 | 0.057(5) | 0.0051(3) | 0.91(2) | $apa_0y$-1 | 0.10(2) | 0.008(2) | 0.91(2) |
| $ApA_1Y$-1 | 0.053(8) | 0.0088(5) | 0.83(1) | $apa_1y$-1 | 0.08(2) | 0.014(3) | 0.83(1) |
| $ApA_2Y$-1 | 0.04(1) | 0.028(8) | 0.45(4) | $apa_2y$-1 | 0.11(1) | 0.042(5) | 0.63(5) |
| $ApA_3Y$-1 | 0.039(7) | 0.031(6) | 0.26(3) | $apa_3y$-1 | 0.12(1) | 0.052(2) | 0.5(1) |
| $ApA_0Y$-2 | 0.031(1) | 0.0024(6) | 0.92(2) | $apa_0y$-2 | 0.042(5) | 0.005(3) | 0.88(1) |
| $ApA_1Y$-2 | 0.024(6) | 0.007(2) | 0.69(3) | $apa_1y$-2 | 0.024(8) | 0.008(3) | 0.65(3) |
| $ApA_2Y$-2 | 0.020(8) | 0.012(3) | 0.38(8) | $apa_2y$-2 | 0.028(7) | 0.013(3) | 0.54(2) |
| $ApA_3Y$-2 | 0.016(6) | 0.016(5) | 0.09(1) | $apa_3y$-2 | 0.039(9) | 0.025(7) | 0.35(4) |
| $ApA_0C$-$YT_1$ | 0.026(6) | 0.023(6) | 0.11(6) | $apa_0c$-$yu_1$ | 0.017(1) | 0.018(4) | 0.1(1) |
| $ApA_1C$-$YT_2$ | 0.015(3) | 0.011(2) | 0.30(5) | $apa_0c$-$yu_2$ | 0.017(1) | 0.011(1) | 0.34(6) |
| $ApA_2C$-$YT_3$ | 0.019(6) | 0.015(3) | 0.22(9) | $apa_0c$-$yu_3$ | 0.028(3) | 0.022(1) | 0.2(1) |
| $ApA_3C$-$YT_4$ | 0.018(1) | 0.016(1) | 0.12(3) | $apa_0c$-$yu_4$ | 0.037(3) | 0.032(1) | 0.13(6) |

[a] Measurements were made using 100 $\mu$M or 50 $\mu$M duplex samples (intrastrand and interstrand CT assemblies, respectively), in 100 mM sodium phosphate buffer pH 7 at 5 °C (Type-1 duplexes) or 10 °C (Type-2 duplexes). The numbers in parentheses represent the standard deviations observed from experiments with three to six different duplex samples generated from at least two independent oligonucleotide syntheses.

A second diagnostic feature of the fluorescence excitation spectra of Ap-containing duplexes is the relative intensity of the short wavelength band (~270 nm). The appearance of this band has been ascribed to singlet−singlet energy transfer from neighboring DNA bases to Ap.[29b,44] The relative intensity of this band is, therefore, associated with the efficiency of energy transfer and has also been used as a measure of base stacking interactions.[29b,44] The variation in the relative intensity of the short wavelength band as a function of increasing *n* in $Ap(A)_nI$-2 DNA duplexes and $ap(a)_ni$-2 DNA:RNA hybrids are presented in Figure 3b and c, respectively. Analogous excitation spectra are observed for the other intra- and interstrand CT assemblies of DNA and DNA:RNA duplexes, including the redox-active duplexes. An increase in intensity and relative energy transfer efficiency is observed as the number of consecutive adenines is increased in both DNA duplexes and DNA:RNA hybrids. This is consistent with recent experiments that find adenine to be the most efficient energy donor and stacks of adenines to behave as funnels for energy transfer to Ap in DNA duplexes.[44a] Significantly, the relative intensity of the energy transfer band and its variation with the number of consecutive adenines are identical in DNA and DNA:RNA duplexes.

**Relative Fluorescence Intensities.** Table 3 compiles the relative fluorescence intensities for steady-state fluorescence emissions of Ap ($\Phi_r$) in the DNA duplexes and DNA:RNA hybrids. An important observation is that $\Phi_r$ is consistently higher in the DNA:RNA hybrids than in the DNA duplexes. This is true both for redox-inactive (I-containing duplexes) and for redox-active (G- or Z-containing) duplexes of Type-1 and Type-2 assemblies. The trends in $\Phi_r$ of redox-inactive duplexes as a function of sequence are significant. For DNA duplexes, $\Phi_r$ is highest in the ApI configurations. For the $Ap(A)_nI$ configurations ($n = 1, 2, 3$), $\Phi_r$ decreases monotonically with increasing numbers of consecutive adenines adjacent to Ap. This decrease in the relative fluorescence intensity of Ap with increasing numbers of adjacent adenines is likely a consequence of a small amount of oxidative CT between Ap* and adenine.[15b] Conversely, for $Ap(A)_nI$ configurations ($n = 1, 2, 3$) in the DNA:RNA hybrids, $\Phi_r$ *increases* monotonically with increasing numbers of consecutive adenines adjacent to Ap. Since oxidative CT between Ap* and A likely also occurs in the DNA:RNA hybrids, additional factors such as increased structural dynamics (vide infra) must play a larger role, leading to an increase in the relative fluorescence intensity with increasing numbers of consecutive adenines. Consequently, the difference in $\Phi_r$ values, $\Delta\Phi_r$, between the DNA:RNA hybrids and the DNA duplexes increases linearly as the number of d(A)−d(T) or d(A)−r(U) base pairs adjacent to Ap increases from one to three.

***Table 4.*** Fluorescence Lifetimes, $\tau_F$, and the Relative Contribution of Each Lifetime to the Total Emission Decay, $\alpha$, of Ap in DNA Duplexes and DNA:RNA Hybrids (100 $\mu$M Duplexes in 100 mM Sodium Phosphate Buffer at pH 7)[a]

| DNA duplex | $\tau_1$/ns ($\alpha_1$) | $\tau_2$/ns ($\alpha_2$) | DNA:RNA duplex | $\tau_1$/ns ($\alpha_1$) | $\tau_2$/ns ($\alpha_2$) | $\Delta\alpha_1$ |
|---|---|---|---|---|---|---|
| $ApA_0I$-2 | 0.77 (0.82) | 6.9 (0.18) | $apa_0i$-2 | 0.84 (0.55) | 6.6 (0.45) | 0.27 |
| $ApA_1I$-2 | 0.87 (0.56) | 7.3 (0.44) | $apa_1i$-2 | 1.1 (0.41) | 7.6 (0.59) | 0.15 |
| $ApA_2I$-2 | 0.74 (0.71) | 6.5 (0.29) | $apa_2i$-2 | 1.0 (0.40) | 7.2 (0.60) | 0.31 |
| $ApA_3I$-2 | 0.78 (0.79) | 6.3 (0.21) | $apa_3i$-2 | 0.95 (0.35) | 7.4 (0.65) | 0.44 |

[a] The values were obtained by fitting the emission decay traces (50 ns total time) to a double first-order exponential expression. The quantity $\Delta\alpha_1$ corresponds to the difference in $\alpha_1$, the fraction of fast decay, DNA − DNA:RNA hybrid.

**Fluorescence Lifetimes.** Parallel trends are revealed when one considers the fluorescence lifetime of Ap ($\tau_F$) in redox-inactive DNA duplexes and DNA:RNA hybrids. It is well-known that the time-resolved fluorescence of Ap* in duplex DNA decays in a multiexponential fashion.[29f,30,39a,b,43] In redox-inactive duplexes, the multiple lifetimes correspond to different modes and/or efficiencies of fluorescence quenching and are related to conformational motions of Ap within the duplex environment. Significantly, these picosecond and nanosecond molecular motions are on the time scale of CT reactions observed in redox-active duplexes containing G or Z. Emission decay, even in redox-inactive duplexes, occurs on significantly shorter time scales than those accessible in the current experiments and is commonly fit using four exponentials.[29f,30,39a,b,43] Here, emission of Ap in DNA and DNA:RNA duplexes was monitored over a 50-ns time regime (IRF ≈ 500 ps). The resultant emission decay was fit to a biexponential expression yielding two lifetimes and their corresponding contributions to the overall decays (Table 4). The lifetimes reported thus correspond to the longer components obtained from fitting the total decay. However, the lifetime data obtained in this time regime clearly confirm that Ap* is longer lived in the DNA:RNA hybrids than in the DNA duplexes (Figure 4). The lifetime enhancement of Ap* within the hybrid duplexes appears to be associated with a greater contribution of the longer lived

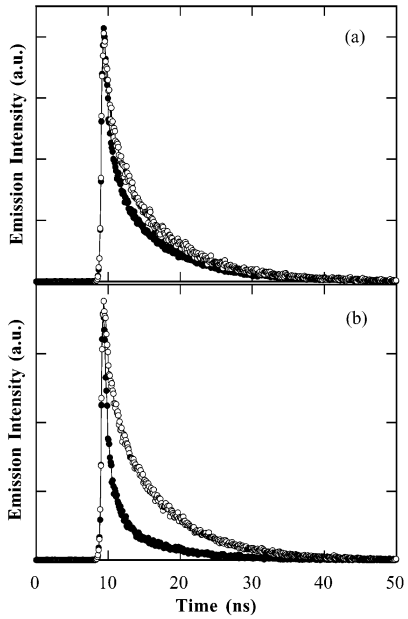


***Figure 4.*** Time-resolved fluorescence of Ap in redox-inactive Type-2 DNA duplexes, $ApA_nI$-2 (closed circles), and DNA:RNA hybrids, $apa_ni$-2, (open circles), following photoexcitation with 355-nm laser light; (a) $n = 1$ and (b) $n = 3$. The decay traces were obtained by monitoring the emission at wavelengths greater than ~370 nm with a streak camera. The instrument response in this time regime was 542 ps.

***Table 5.*** Fluorescence Polarization of Ap in DNA Duplexes and DNA:RNA Hybrids and the Percent Difference in Polarization, $\Delta P$ ($\Delta P = 100[P_{DNA} - P_{hybrid}]/P_{DNA}$), between the Two Duplexes[b]

| DNA duplex | polarization Y = I | polarization Y = G | DNA:RNA duplex | polarization Y = I | polarization Y = G | Δpolarization Y = I (%) |
|---|---|---|---|---|---|---|
| $ApA_0Y$-2 | 0.36 | na[a] | $apa_0y$-2 | 0.33 | na | 8 |
| $ApA_1Y$-2 | 0.27 | 0.28 | $apa_1y$-2 | 0.23 | 0.24 | 15 |
| $ApA_2Y$-2 | 0.29 | 0.35 | $apa_2y$-2 | 0.21 | 0.25 | 28 |
| $ApA_3Y$-2 | 0.37 | 0.26 | $apa_3y$-2 | 0.20 | 0.21 | 46 |
| $ApA_0C$-$YT_1$ | 0.38 | 0.39 | $apa_0a$-$yu_1$ | 0.25 | 0.36 | 35 |
| $ApA_1C$-$YT_2$ | 0.33 | 0.39 | $apa_1a$-$yu_2$ | 0.23 | 0.26 | 32 |
| $ApA_2C$-$YT_3$ | 0.36 | 0.35 | $apa_2a$-$yu_3$ | 0.19 | 0.23 | 45 |
| $ApA_3C$-$YT_4$ | 0.37 | 0.38 | $apa_3a$-$yu_4$ | 0.19 | 0.21 | 47 |

[a] Because of the significant CT quenching of the fluorescence signal from ApG/apg duplexes, an accurate fluorescence polarization cannot be obtained for these samples. [b] Measurements were made using 100 $\mu$M or 50 $\mu$M (intrastrand and interstrand CT assemblies, respectively) duplex samples in 100 mM sodium phosphate buffer at pH 7 at 10 °C.

component to the total decay, rather than a significant increase in the absolute magnitude of one of the fluorescence lifetimes. Furthermore, the difference in fluorescence lifetimes between the DNA duplexes and the DNA:RNA hybrids increases with the number of consecutive d(A)−d(T) or d(A)−r(U) base pairs adjacent to Ap. This is likewise consistent with steady-state fluorescence measurements.

**Fluorescence Polarization.** Studies of Ap fluorescence polarization in oligonucleotides can provide additional confirmation that Ap is incorporated within the duplex and are an added probe of flexibility. Very low fluorescence polarization is found for Ap in solution (<0.005) and for the poorly stacked DNA base analogue, 1,$N^6$-ethenoadenine, within DNA duplexes (~0.01).[15c] In contrast, significant steady-state fluorescence polarization is observed for Ap in all DNA duplexes and DNA:RNA hybrids employed here (Table 5). These levels of polarization (~0.2−0.4) are consistent with previous investigations of Ap-containing DNA duplexes[15c,39a,b] and indicate that

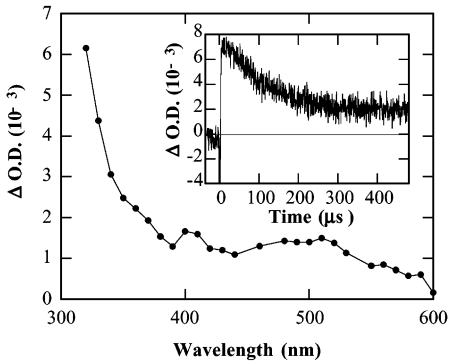


***Figure 5.*** Transient absorption spectrum upon nanosecond laser photolysis (310 nm) of an aerated solution of 100 $\mu$M Ap and 50 mM dGTP in 100 mM sodium phosphate buffer at pH 7. Inset shows the decay trace monitored at 320 nm.

Ap is base paired and stacked within both DNA duplexes and DNA:RNA hybrids. Notably, however, the polarization values are consistently lower in the DNA:RNA hybrids than in the analogous DNA duplexes. Moreover, consistent with earlier trends, the difference in fluorescence polarizations between the DNA duplexes and the DNA:RNA hybrids, $\Delta P$, increases systematically as the number of consecutive d(A)−d(T) or d(A)−r(U) base pairs increases.

**Investigations of CT.** In solution, the fluorescence of Ap* is efficiently quenched by the nucleotides dGTP and dZTP with rate constants of $2.2 \times 10^9$ $M^{-1}$ $s^{-1}$ and $5.2 \times 10^9$ $M^{-1}$ $s^{-1}$, respectively.[15c] This fluorescence quenching has been attributed to electron transfer from the free nucleotides to Ap*, and the quenching rate constants parallel the driving force for ET. Also consistent with this interpretation is the fact that the corresponding CT reaction with dITP, which is thermoneutral, is not observed to any significant extent. In addition, quenching via energy transfer can realistically be ruled out because of the lack of spectral overlap between the fluorescence of photoexcited Ap and the absorption of the natural DNA bases.

**Transient Absorption Measurements with dGTP.** Confirmation that ET occurs between Ap* and dGTP in solution is obtained from transient absorption experiments (Figure 5). The transient spectrum observed upon nanosecond laser photolysis of solutions containing Ap and dGTP exhibits a strong, sharp positive absorption near 320 nm and broad weaker absorption between 400 and 600 nm. This spectrum is highly reminiscent of that of the neutral guanine radical[21d,50] and is distinct from that of the guanine radical cation; the guanine radical cation, the initial product of ET between Ap* and dGTP, is known to rapidly deprotonate in solution.[50] Observation of the guanine radical in the microsecond time regime is due to the small fraction of ET-generated guanine radical cations which escape back via ET and deprotonate to the neutral species. Because of the broad, featureless absorption spectrum of the guanine radical, monitoring base−base CT reactions by transient absorption is difficult, particularly in duplex DNA. Consequently, we have probed base−base CT reactions in Ap-containing oligonucleotide duplexes with fluorescence techniques.

**Calibration of CT.** The challenge in studies of DNA CT involving Ap*, therefore, is not establishing that CT occurs in DNA but delineating quenching due to CT from quenching due

(50) Candeias, L. P.; Steenken, S. *J. Am. Chem. Soc.* **1989**, *111*, 1094−1099.

to other interactions of Ap* in the DNA environment. This "non-CT" quenching is dramatically evident by the reduction in the fluorescence intensity and lifetime of Ap* in DNA duplexes, even redox-inactive assemblies, compared to free Ap in solution. Our method for delineating CT from other modes of fluorescence quenching involves calibrating the fluorescence in redox-active duplexes against those of otherwise identical duplexes, where the electron donor, G or Z, is replaced by a redox-inactive analogue, I. In this way, the amount of quenching due to the exchange of G or Z for I is determined. That this quenching is due to CT is based on the premise that exchange of a single G or Z for I induces a major perturbation in CT driving force (200 or 500 mV for G or Z, respectively) but a correspondingly minor perturbation in structure. Certainly, the duplexes substituted with I are not *identical* to the duplexes containing G or Z. Thus, we cannot realistically argue that 100% of the fluorescence quenching is due to CT. The exchange of G or Z for I results in the loss of the exocyclic amino group in the minor groove and, more importantly for our studies, the loss of one H bond in the base pair with C. Thus, substitution of an I−C base pair for a G−C base pair reduces the melting temperature of the duplex by a few degrees and may enhance base dynamics at or near the I site. However, the structural consequences of a single I substitution are relatively minor, as evidenced by crystal structures[51] and theoretical investigations.[52] In fact, the close similarities we observe in the CD spectra, fluorescence excitation spectra, and fluorescence polarization between analogous G or Z and I duplexes strongly suggest that differences in base stacking, structure, and dynamics are not significant. Certainly, the structural perturbations are not as large as the electronic perturbations, which are responsible for CT, and these dominate the observed quenching.

**Time-Resolved and Steady-State Measurements.** The time-resolved fluorescence data for Ap-containing assemblies presented in Figure 6 demonstrate that the fluorescence decay is faster in the redox-active G-containing duplexes than in the redox-inactive I-containing duplexes. The multicomponent decay of Ap fluorescence in oligonucleotide duplexes can also be seen. Our previous investigations of base−base CT involving Ap* demonstrate that intrastrand CT reactions are extremely rapid ($k = 10^9-10^{11}$ s$^{-1}$) over these distances.[15b,c] Here, the time resolution is insufficient to observe most of the fast decay components in the redox-active duplexes, and consequently, it is not possible to quantitatively measure these fluorescence decay rate constants. Therefore, the yield of CT in DNA and DNA:RNA duplexes was investigated using steady-state fluorescence measurements.

The yield of CT between either G or Z and Ap* was determined by comparing the emission spectra of Ap* in redox-active G- or Z-containing duplexes to those of otherwise identical duplexes in which the G or Z is replaced by I. Hence, fluorescence quenching due to CT is quantified as $F_q$ ($F_q = 1 - \Phi_{rG/Z}/\Phi_{rI}$). The yields of intra- and interstrand CT quenching of photoexcited Ap in DNA and DNA:RNA duplexes are shown in Table 3.

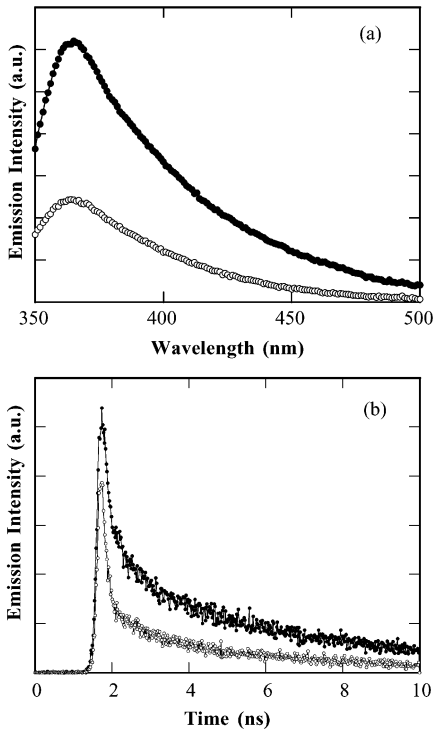


***Figure 6.*** (a) Steady-state emission spectra of 100 $\mu$M DNA:RNA duplexes, apa$_1$i-2 (closed circles) and apa$_1$g-2 (open circles), in 100 mM sodium phosphate buffer at pH 7 and 10 °C. (b) Time-resolved emission decay traces of 100 $\mu$M DNA duplexes, ApA$_1$I-2 (closed circles) and ApA$_1$G-2 (open circles), in 100 mM sodium phosphate buffer at pH 7.

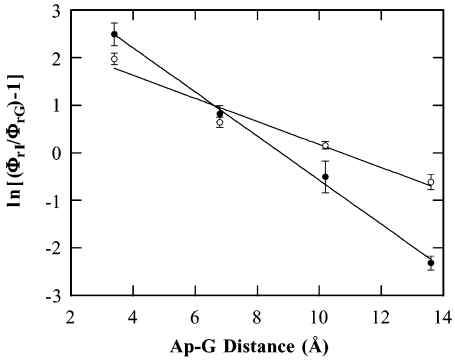


***Figure 7.*** Variation in the yield of intrastrand charge transfer (as obtained from steady-state fluorescence measurements) as a function of distance observed in Type-2 DNA duplexes (closed circles) and DNA:RNA hybrids (open circles).

Several striking results emerge. First, the CT quenching efficiency in DNA:RNA hybrids is similar to, and in many cases greater than, that in DNA duplexes. Second, $\Delta F_q$, the difference in $F_q$ values between the DNA and the DNA:RNA duplexes, increases with the increasing number of A−T/A−U base pairs separating Ap from the electron donor. Third, the variation in yields of CT quenching as a function of distance is different in the DNA and DNA:RNA hybrid duplexes. A plot (Figure 7) of the natural logarithm of CT emission quenching against donor−acceptor distance provides a dramatic demonstration of this difference between DNA and DNA:RNA duplexes. The slopes of this plot, $\gamma$, which represents the distance dependence of CT yield,[15c] are found to be 0.45 ± 0.02 Å$^{-1}$ and 0.20 ± 0.02 Å$^{-1}$ for intrastrand CT in Type-2 DNA and DNA:RNA duplexes, respectively. A similar trend was observed for the Type-1

(51) (a) Xuan, J.-C.; Weber, I. T. *Nucleic Acids Res.* **1992**, *20*, 5457−5464. (b) Lipanov, A.; Kopka, M. L.; Kaczor-Grzeskowiak, M.; Quintana, J.; Dickerson, R. E. *Biochemistry* **1993**, *32*, 1373−1389.
(52) Cuberno, E.; Güimil-García, R.; Luque, F. J.; Eritja, R.; Orozco, M. *Nucleic Acids Res.* **2001**, *29*, 2522−2534.

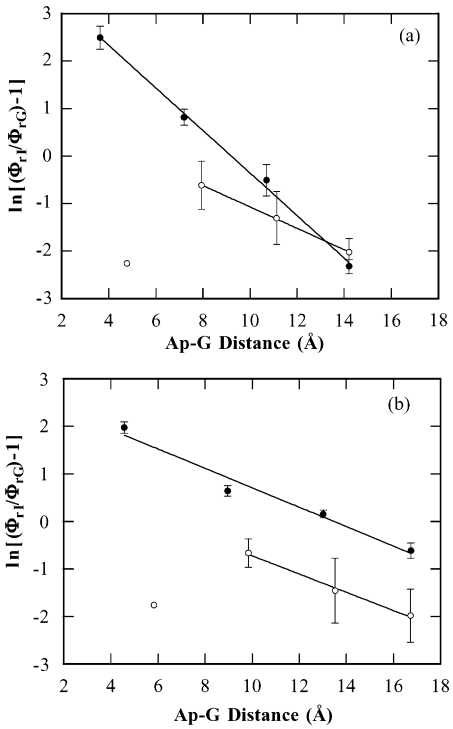


***Figure 8.*** Variation in the yield of intrastrand charge transfer (closed circles) and interstrand charge transfer (open circles) (as obtained from steady-state fluorescence measurements) as a function of distance in (a) Type-2 DNA duplexes and (b) Type-2 DNA:RNA hybrid duplexes.

assemblies, where $\gamma$ was found to be $0.35 \pm 0.04$ Å$^{-1}$ for CT in DNA duplexes and $0.21 \pm 0.03$ Å$^{-1}$ for CT in DNA:RNA hybrids.

The trends in intra- versus interstrand CT processes are distinct in DNA and DNA:RNA hybrids. Similar to our previous report,[15c] interstrand CT in B-DNA is characterized by a significantly lower efficiency but an overall distance dependence ($\gamma = 0.22 \pm 0.01$ Å$^{-1}$) which is more shallow (Figure 8a). In the DNA:RNA hybrids, although the interstrand quenching efficiency is found to be somewhat reduced, the overall distance dependence ($\gamma = 0.19 \pm 0.01$ Å$^{-1}$) is essentially identical for the intra- and interstrand reactions (Figure 8b).

## Discussion

**Ap* Fluorescence in Nucleic Acid Duplexes.** Various mechanisms and/or conditions, including stacking,[39a,43] hydrogen bonding,[37b,40] base−base collisions,[43] and CT reactions[15b,c,30] have been proposed to explain the quenching of Ap* fluorescence upon incorporation in DNA. Our current investigations distinguish CT from other modes of fluorescence quenching by examining the fluorescence in analogous redox-active and redox-inactive duplexes. However, to strengthen these CT investigations we have also considered how the sequence-dependent structure and dynamics of the redox-inactive DNA and DNA:RNA duplexes influence the behavior of Ap*. A significant theme emerging from these studies is the importance of nucleic acid structural dynamics on various features of Ap* fluorescence. The motions of Ap between various conformational states in DNA generate a strongly heterogeneous and dynamic environment, as attested to by the pronounced nonexponentiality of Ap* fluorescence decay in DNA.[29f,30,39a,b,43] This dynamic exchange between conformational states modulates stacking, H bonding, and other base−base interactions on the fluorescence time-scale and is, thereby, essential to fluorescence quenching irrespective of the specific mechanism(s). The photophysics of Ap can thus be described in terms of a model, where the DNA bases move relative to one another,[39a] leading to different degrees of fluorescence quenching. We consider that these motions, which regulate quenching mechanisms in redox-inactive duplexes, are equally and similarly important to quenching via CT. In this way, the sensitivity of Ap* fluorescence to these dynamics renders it a reporter of structural dynamics, CT, and their relationship.

**Structure and Structural Dynamics of Ap and the d(A)−d(T) or d(A)−r(U) Motifs within DNA and DNA:RNA Duplexes.** The spectroscopic investigations described here can be utilized in characterizing the structure and structural dynamics of the Ap-containing DNA duplexes and DNA:RNA hybrids. It should be emphasized first that the spectroscopic evidence consistently indicates that Ap is included within both DNA and DNA:RNA duplexes and participates in hydrogen bonding and stacking interactions in a manner analogous to adenine. The relative fluorescence intensities, fluorescence lifetimes, and polarization as well as the $T_m$ values of the current DNA assemblies indicate that substitution of Ap−T for A−T base pairs causes minimal perturbation in DNA structure.[37,39a,c,44] Furthermore, the absorption, emission, and excitation spectra as well as fluorescence polarization of Ap in DNA:RNA hybrids indicate that Ap is also incorporated within the base stack of these duplexes.[40,53] The general photophysical characteristics of Ap in DNA:RNA duplexes are similar to those of Ap in DNA duplexes.

Specific differences in the spectroscopic parameters and thermal stability between our DNA and DNA:RNA duplexes may be attributed to differences in structure and structural dynamics (vide infra) of the duplexes, rather than perturbations at the Ap site. For instance, the close similarity between the excitation spectra of the DNA duplexes and the DNA:RNA hybrids strongly suggests that Ap is similarly stacked within the two duplex environments. Furthermore, the lower $T_m$ values of the DNA:RNA hybrids (obtained by monitoring Ap absorbance) are not associated with poor inclusion of Ap within the duplex structure. The reduction in $T_m$ is in agreement with the behavior of DNA:RNA hybrids that do not contain Ap.[33b,42,48] Furthermore, duplexes that contain a perturbation at Ap, such as Ap at a mismatch[15c,37a] or strand termini,[29f] do not exhibit the cooperative melting transitions and the hypochromicities observed here.

Both CD and NMR spectroscopy establish that the DNA:RNA hybrids are structurally distinct from the DNA duplexes and that the hybrids possess a global structure which is predominantly A-form. Significantly, one structural feature that distinguishes A- and B-helices is the difference in intra- versus interstrand base stacking. In particular, while base overlap in B-helices is largely limited to interactions between bases on the same strand, overlap in A-helices also involves bases belonging to different strands. This interstrand overlap in A-helices is a consequence of the low twist, which favors both intra- and interstrand interactions, and the large, positive tilt, which increases interstrand overlap.[31] Consistent with this stacking in A- and B-helices are the base−base surface overlaps

(53) Janion, C.; Shugar, D. *Acta Biochim. Pol.* **1973**, *20*, 271−284.

determined for idealized dinucleotides of DNA and DNA:RNA hybrids.[28e] Similar intrastrand overlap is observed for DNA and DNA:RNA hybrids, particularly for the extremely well-stacked purine−purine steps. Conversely, interstrand overlap, which is essentially negligible for all base steps in B-form DNA, is appreciable in the A-form DNA:RNA hybrids, particularly between purines of pyrimidine−purine steps.

Although stacking is a complex intermolecular interaction which cannot be completely described by empirical parameters, such as physical overlap, trends in stacking energies determined both experimentally[29b,44,54] and theoretically[55] are consistent with the intuitive correlation between base overlap and stacking. One experimental probe of base stacking interactions is energy transfer from natural DNA bases to Ap in DNA oligomers and DNA duplexes.[29b,44a] Investigations of energy transfer in DNA and DNA:RNA hybrids presented in the current work suggest that strong stacking interactions exist in the DNA:RNA hybrids, similar to those in the B-DNA duplexes. Although these experiments cannot distinguish between intra- and interstrand contributions, the results are consistent with expectations on the basis of the similar total base−base overlap of idealized dinucleotide steps in DNA and DNA:RNA duplexes.[28e]

In addition to the distinct static structural features of DNA duplexes and DNA:RNA hybrids, photophysical investigations suggest that the structural dynamics are also significantly different. Structural dynamics, such as spontaneous fluctuations of the structure about the average, are an integral feature of DNA in solution, for which an ensemble of energetically similar conformational states exist. Sequence-dependent structural dynamics are, therefore, crucial to the physical and chemical behavior of nucleic acid helices. Motion of the DNA bases is fundamental to DNA structural dynamics, and recent fluorescence measurements have observed picosecond and nanosecond motion of bases in DNA.[39a,b,56]

Our photophysical measurements in DNA:RNA and DNA duplexes indicate that Ap is significantly more mobile in the DNA:RNA hybrids than in the DNA duplexes. As a result of this enhanced mobility, Ap likely undergoes more rapid exchange between conformational states or samples a larger variety of conformational states in the DNA:RNA hybrids than in DNA duplexes. This is exemplified by the higher relative fluorescence intensities and longer fluorescence lifetimes of Ap within the DNA:RNA hybrids. Because of the increased conformational freedom, Ap is less rigidly fixed in DNA:RNA hybrids, samples the surrounding aqueous media more often, and displays fluorescence features more heavily influenced by this external environment. Steady-state fluorescence polarization also suggests enhanced Ap mobility in the DNA:RNA hybrids, although the longer fluorescence lifetime contributes to the reduced polarization.

Photophysical investigations consistently suggest that the enhanced conformational freedom of Ap in the DNA:RNA hybrids extends to the neighboring bases, in particular to the Ap(A)$_n$Y motif. Thus, the differences in $T_m$ values, hypochromicity, relative fluorescence intensity, fluorescence lifetime, and fluorescence polarization between the DNA duplexes and the DNA:RNA hybrids increase systematically with $n$, the number of consecutive d(A)−d(T) or d(A)−r(U) base pairs adjacent to Ap. Significantly, this trend is not related to the substitution of T by U in purely B-form DNA. Thus, the Ap(A)$_n$Y motif (including the complementary base pairs) is less rigid and more mobile and has access to a greater population of conformations in the DNA:RNA hybrids than that in the DNA duplexes.

The notion that DNA:RNA hybrids and, indeed, specific sequence regimes in these structures may exhibit enhanced conformational freedom relative to analogous DNA duplexes is consistent with several previous reports. For instance, investigations of sequence-dependent variations in oligonucleotide stability reveal striking differences between DNA, RNA, and DNA:RNA duplexes exacerbated by specific sequences.[42] The d(A)−r(U) configuration and, especially, d(A)$_n$−r(U)$_n$ tracts appear to be particularly destabilizing. Analogous observations have been made regarding the mobility of r(A−U) base pairs from evaluations of base pair lifetimes in RNA duplexes.[34a] Thus, while the lifetimes of r(G−C) base pairs (∼30−50 ms) are similar, or even longer than those of d(G−C) base pairs, the r(A−U) base pair lifetimes (≤0.1 ms) are dramatically shorter than d(A−T) lifetimes (∼0.5−7 ms). Furthermore, this difference is explicitly associated with the A-RNA structure and is not related to the substitution of T by U.

Several factors may be responsible for the enhanced base flexibility of the Ap(A)$_n$Y motif within the DNA:RNA hybrid structure, including weakened hydrogen bonding, reduced stacking interactions, or a combination of the two. Significantly, however, experimental investigations of energy transfer, which probe stacking interactions, observe energy transfer efficiencies to be virtually identical in the DNA and DNA:RNA duplexes. This suggests that reduced hydrogen bonding interactions between the base pairs is primarily responsible for the increased flexibility of the DNA:RNA hybrids. Consistent with this suggestion are the short lifetimes of r(A−U) base pairs in RNA duplexes. Reduced hydrogen bond strength in DNA:RNA hybrids also correlates with the picture of the A-form structure as a wide, compact helix, where the bases of each strand are displaced off the helical axis.

**Charge Transfer is Regulated by Structural Dynamics.** The distance dependence of intrastrand CT yield in DNA:RNA hybrids, $\gamma$, is significantly more shallow than that in DNA duplexes (Figure 7). Aside from the conformational differences originating from the ribose sugars, the DNA and DNA:RNA CT assemblies are structurally identical. Indeed, apart from minor differences in the bridge resulting from substitution of U for T, the overall CT energetics are also maintained between these two forms. Thus, the striking difference in the distance dependence of intrastrand CT must be correlated to the distinctions in structure and structural flexibilities that arise. Significantly, the difference in CT efficiency in the DNA:RNA hybrids and DNA duplexes parallels the difference in the mobility of the Ap(A)$_n$Y motif within these structures. As the flexibility is increased in the hybrids relative to the DNA

(54) (a) Kool, E. T. *Annu. Rev. Biophys. Biomol. Struct.* **2001**, *30*, 1−22. (b) Guckian, K. M.; Schweitzer, B. A.; Ren, R. X. F.; Sheils, C. J.; Tahmassebi, D. C.; Kool, E. T. *J. Am. Chem. Soc.* **2000**, *122*, 2213−2222. (c) Bommarito, S.; Peyret, N.; SantaLucia, J. *Nucleic Acids Res.* **2000**, *28*, 1929−1934.
(55) (a) Sponer, J.; Berger, I.; Spackova, N.; Leszczynski, J.; Hobza, P. *J. Biomol. Struct. Dyn.* **2000**, 383−407. (b) Hobza, P.; Sponer, J. *Chem. Rev.* **1999**, *99*, 3247−3276. (c) Sponer, J.; Leszczynski, J.; Hobza, P. *J. Biomol. Struct. Dyn* **1996**, *14*, 117−135.
(56) (a) Brauns, E. B.; Murphy, C. J.; Berg, M. A. *J. Am. Chem. Soc.* **1998**, *120*, 2449−2456. (b) Brauns, E. B.; Madaras, M. L.; Coleman, R. S.; Murphy, C. J.; Berg, M. A. *J. Am. Chem. Soc.* **1999**, *121*, 11644−11649.

duplexes, the difference in CT efficiency between the two duplexes increases. Here, the DNA:RNA duplexes, which possess more mobility, exhibit enhanced CT efficiency.

The more shallow distance dependence in DNA:RNA hybrids versus DNA duplexes can be rationalized in terms of the relationship between structural flexibility and CT efficiency and the notion that specific conformations are active toward CT.[15d] Because of the enhanced mobility of the d(A)−r(U) bases within the DNA:RNA hybrids, these duplexes have greater access to conformations and, therefore, a higher probability of achieving CT-active conformations. Clearly, in the extreme, large structural fluctuations lead to base destacking with a concomitant reduction in CT yield. In fact, with increasing temperature, an increase in CT efficiency has been observed for both rhodium[2b] and ethidium intercalators[15f] before reaching the temperature regime associated with duplex melting and diminished CT efficiency. It does not seem unreasonable, therefore, to suggest that there exists a level of structural fluctuations which are optimal for CT efficiency. One explanation for the difference in $\gamma$ values for these DNA and DNA:RNA duplexes is that the $Ap(A)_nY$ motif within the DNA assemblies is below the optimal level for CT, whereas increased conformational fluctuation in the DNA:RNA hybrids results in more efficient CT over longer distances.

Several recent theoretical models suggest the importance of DNA dynamics to DNA-mediated CT.[8a,9−11] For instance, Rudnick and co-workers treat CT as classical diffusion along a chain under conditions of large amplitude structural fluctuations and propose that these thermally induced fluctuations are required, rate-limiting steps in CT.[9] In this model, CT is described in terms of a repeated series of reversible redox reactions, where each step must overcome a transition-state barrier, as in a classical chemical reaction. To proceed through the transition state, the system must obtain an optimum geometric configuration for CT. The thermally induced structural fluctuations, thereby, facilitate CT by providing access to these conformations. Likewise, Smith and Adamowicz invoke fluctuation geometries of thymine bases to transport electrons through d(A−T) duplexes.[11]

**Intra- and Interstrand Charge-Transfer Processes are Distinct.** Using base−base CT reactions, we have previously seen that intra- and interstrand CT processes are characterized by different efficiencies, different rate constants, and different mechanistic pathways.[15c] The intra- and interstrand CT reactions examined in the current work further emphasize these differences, suggesting that they are a general trend and not specific to a particular B-DNA sequence. In particular, the yields of interstrand CT in DNA duplexes are significantly lower than the yields of the corresponding intrastrand reactions, although the interstrand distance dependence is more shallow (Figure 8a), consistent with previous observations. Note that the strikingly low yield for CT in the DNA and DNA:RNA duplexes $ApA_0C$-$YT_1$ and $apa_0c$-$yu_1$ is likely related to a reductive CT reaction between Ap* and the adjacent C.[15b] Interestingly, the dominance of intrastrand over interstrand CT processes was also recently demonstrated for guanine oxidation in B-DNA duplexes following high energy ionization.[57]

These experimental results are consistent with the differences in intra- and interstrand base stacking characteristic of B-DNA duplexes, as assessed from base overlap, as described above, but contrast with recent theoretical calculations of electronic coupling between DNA bases.[58] Such calculations find appreciable interstrand electronic coupling between several bases, for instance A and G, and particularly between A bases, for which interstrand couplings are predicted to be, in some cases, comparable to intrastrand couplings. It appears that these electronic couplings, calculated for static, isolated DNA base pair dimers or trimers, do not completely correlate with experimental evaluations of CT efficiencies in large DNA duplexes at finite temperatures. This could be attributed to several significant parameters which are not readily incorporated into theoretical treatments including cooperativity effects, solvation, the effect of photoexcitation, and certainly structural dynamics. Significantly, dramatic variations in electronic coupling as a function of typical DNA dynamical motion have recently been demonstrated theoretically.[59] We are currently examining base−base CT in other DNA assemblies in order to obtain more experimental data which address these issues.

Perhaps an even more revealing comment on the differences between intra- and interstrand reactivity emerges from a comparison of the DNA duplexes and the DNA:RNA hybrids. Although interstrand CT reactions in B-DNA are significantly less distance dependent than their intrastrand counterparts (Figure 8a), the distance dependences of the intra and interstrand reactions in the DNA:RNA hybrids are essentially identical (Figure 8b). This similarity in distance dependences of CT yield via intra- and interstrand pathways in DNA:RNA hybrids is consistent with the appreciable interstrand stacking overlap in these duplexes. Thus, while CT, which is modulated by stacking, is specific to an intrastrand pathway in B-DNA, interstrand overlap in A conformations may facilitate rapid charge equilibration between the two strands of the DNA:RNA hybrid. If so, the differences between intra- and interstrand CT processes observed in B-DNA[15c] may not be so dramatic in the A-form DNA:RNA hybrids. Indeed, this is observed in the present work.

**Implications.** DNA-mediated CT has now been seen through many different experiments to depend sensitively upon nucleic acid structure.[2,15,21,28] The spectroscopic investigations of base−base CT presented here emphasize the importance of structure to DNA CT and establish that structural dynamics influence charge injection and CT processes explicitly. Significantly, comparative studies of base−base CT in these DNA and analogous DNA:RNA duplexes reveal the dramatic impact of relatively minor differences in the structural dynamics of DNA base pairs on CT reactions through DNA. As studies of DNA CT continue to focus on mechanistic details, it is becoming increasingly important to recognize and define the role of subtle structural variations in these reactions. We believe that a significant effect of such structural variations is a modulation of base stacking interactions and, therefore, CT efficiency. The modulated efficiencies of intra- and interstrand CT observed

(57) O'Neill, P.; Parker, A. W.; Plumb, M. A.; Siebbeles, L. D. A. *J. Phys. Chem. B* **2001**, *105*, 5283−5290.

(58) (a) Voityuk, A. A.; Rösch, N.; Bixon, M.; Jortner, J. *J. Phys. Chem. B* **2000**, *104*, 9740−9745. (b) Voityuk, A. A.; Jortner, J.; Bixon, M.; Rösch, N. *J. Chem. Phys.* **2001**, *114*, 5614−5620. (c) Troisi, A.; Orlandi, G. *Chem. Phys. Lett.* **2001**, *344*, 509−518. (d) Brunaud, G.; Castet, F.; Fritsch, A.; Kreisser, M.; Ducasse, L. *J. Phys. Chem. B* **2001**, *105*, 12665−12673.

(59) (a) Voityuk, A. A.; Siriwong, K.; Rösch, N. *Phys. Chem. Chem. Phys.* **2001**, *3*, 5421−5425. (b) Troisi, A.; Orlandi, G. *J. Phys. Chem. B* **2002**, *106*, 2093−2101.

through the d(A)−d(T) and d(A)−r(U) motifs of the B-DNA and A-DNA:RNA duplexes are completely consistent with this mechanistic picture of CT through the dynamic stack of DNA bases.

**Acknowledgment.** We gratefully acknowledge the National Institutes of Health for financial support of this work (GM49216). We also thank the Natural Sciences and Engineering Research Council of Canada (NSERC) for a postdoctoral fellowship (M.A.O.). We appreciate the assistance of Prat Bhattacharya, Eric Stemp, and Julia Lyubovitsky with NMR experiments, nanosecond transient absorption, and picosecond fluorescence measurements, respectively.

**Supporting Information Available:** Table of representative yields and expected and observed molecular masses as determined by MALDI mass spectrometry, for single strand DNA syntheses. Representative melting curves for Ap-containing DNA and DNA:RNA duplexes. Additional CD spectra of Ap-containing DNA and DNA:RNA duplexes. This material is available free of charge via the Internet at http://pubs.acs.org.

JA0208198